Article

A non-hallucinogenic psychedelic analogue with therapeutic potential

https://doi.org/10.1038/s41586-020-3008-z

Received: 17 January 2020

Accepted: 30 October 2020

Published online: 09 December 2020

Check for updates

Lindsay P. Cameron[1], Robert J. Tombari[2], Ju Lu[3], Alexander J. Pell[2], Zefan Q. Hurley[2], Yann Ehinger[4], Maxemiliano V. Vargas[1], Matthew N. McCarroll[5], Jack C. Taylor[5], Douglas Myers-Turnbull[5,6], Taohui Liu[3], Bianca Yaghoobi[7], Lauren J. Laskowski[8], Emilie I. Anderson[8], Guoliang Zhang[2], Jayashri Viswanathan[2], Brandon M. Brown[9], Michelle Tjia[3], Lee E. Dunlap[2], Zachary T. Rabow[10], Oliver Fiehn[10], Heike Wulff[9], John D. McCorvy[8], Pamela J. Lein[7], David Kokel[5,11], Dorit Ron[4], Jamie Peters[12,13], Yi Zuo[3] & David E. Olson[2,14,15,16]✉

The psychedelic alkaloid ibogaine has anti-addictive properties in both humans and animals[1]. Unlike most medications for the treatment of substance use disorders, anecdotal reports suggest that ibogaine has the potential to treat addiction to various substances, including opiates, alcohol and psychostimulants. The effects of ibogaine—like those of other psychedelic compounds—are long-lasting[2], which has been attributed to its ability to modify addiction-related neural circuitry through the activation of neurotrophic factor signalling[3,4]. However, several safety concerns have hindered the clinical development of ibogaine, including its toxicity, hallucinogenic potential and tendency to induce cardiac arrhythmias. Here we apply the principles of function-oriented synthesis to identify the key structural elements of the potential therapeutic pharmacophore of ibogaine, and we use this information to engineer tabernanthalog—a water-soluble, non-hallucinogenic, non-toxic analogue of ibogaine that can be prepared in a single step. In rodents, tabernanthalog was found to promote structural neural plasticity, reduce alcohol- and heroin-seeking behaviour, and produce antidepressant-like effects. This work demonstrates that, through careful chemical design, it is possible to modify a psychedelic compound to produce a safer, non-hallucinogenic variant that has therapeutic potential.

Ibogaine is the most abundant of the numerous alkaloids produced by *Tabernanthe iboga*[5]. Although it has not been tested in double-blind, placebo-controlled clinical trials, anecdotal reports and open-label studies suggest that it can reduce symptoms of drug withdrawal, reduce drug cravings and prevent relapse[1,6]. However, the potential of ibogaine as a therapeutic is limited by several major issues. First, access to large quantities is limited, both by overexploitation of the plant from which it is derived and by the lack of a scalable, enantioselective, total synthesis[6]. Currently, there are only three synthetic routes to racemic ibogaine, with longest linear sequences of between 9 and 16 steps and overall yields that range from 0.1 to 4.8%[6]. Second, the safety profile of ibogaine is unacceptable. It is very non-polar, which leads to its accumulation in adipose tissue[7] and contributes to its known cardiotoxicity through the inhibition of hERG potassium channels[8,9]. Several deaths have been linked to the cardiotoxicity of ibogaine[10,11], and it induces hallucinations that can last for more than 24 hours. Although ibogaine was once sold in France as a medicine for the treatment of neuropsychiatric diseases, it was removed from the market owing to its adverse effects[1].

Although the exact mechanism of action of ibogaine has not yet been fully elucidated, evidence suggests that it might alter addiction-related circuitry by promoting neural plasticity. First, ibogaine has been shown to increase the expression of glial cell-line-derived neurotrophic factor (GDNF) in the ventral tegmental area, and infusion of ibogaine into this region of the midbrain reduces alcohol-seeking behaviour in rodents[3]. A more recent study demonstrated that ibogaine affects brain-derived neurotrophic factor and GDNF signalling in several brain regions that are implicated in the behavioural effects of addictive drugs[4]. Recently, we demonstrated that noribogaine—an active metabolite of ibogaine[12]—is a potent psychoplastogen[13] that increases the complexity of cortical neuron dendritic arbors[14]. Other psychoplastogens—such as lysergic

[1]Neuroscience Graduate Program, University of California, Davis, Davis, CA, USA. [2]Department of Chemistry, University of California, Davis, Davis, CA, USA. [3]Department of Molecular, Cell and Developmental Biology, University of California, Santa Cruz, Santa Cruz, CA, USA. [4]Department of Neurology, University of California, San Francisco, San Francisco, CA, USA. [5]Institute for Neurodegenerative Diseases, University of California, San Francisco, San Francisco, CA, USA. [6]Quantitative Biosciences Consortium, University of California, San Francisco, San Francisco, CA, USA. [7]Department of Molecular Biosciences, School of Veterinary Medicine, University of California, Davis, Davis, CA, USA. [8]Department of Cell Biology, Neurobiology, and Anatomy, Medical College of Wisconsin, Milwaukee, WI, USA. [9]Department of Pharmacology, School of Medicine, University of California, Davis, Davis, CA, USA. [10]West Coast Metabolomics Center, University of California, Davis, Davis, CA, USA. [11]Department of Physiology, University of California, San Francisco, San Francisco, CA, USA. [12]Department of Anesthesiology, University of Colorado Denver, Anschutz Medical Campus, Aurora, CO, USA. [13]Department of Pharmacology, University of Colorado Denver, Anschutz Medical Campus, Aurora, CO, USA. [14]Department of Biochemistry and Molecular Medicine, School of Medicine, University of California, Davis, Sacramento, CA, USA. [15]Center for Neuroscience, University of California, Davis, Davis, CA, USA. [16]Delix Therapeutics, Inc., Palo Alto, CA, USA. ✉e-mail: deolson@ucdavis.edu

acid diethylamide (LSD) and psilocin (the active metabolite of psilocybin)—have also been shown in anecdotal and open-label studies to decrease drug use in the clinic, similar to ibogaine[15]. We suggest that the ability of psychoplastogens to promote structural and functional neural plasticity in addiction-related circuitry might explain their ability to reduce drug-seeking behaviour for weeks to months after a single administration. Moreover, by modifying neural circuitry rather than simply blocking the targets of a particular addictive substance, psychoplastogens such as ibogaine could have the potential for broad use as anti-addictive agents, applicable to the treatment of addiction to various substances.

To develop simplified, and potentially safer, analogues of ibogaine we first needed to understand which of its structural features were critical for its psychoplastogenic effects. Our approach was similar to seminal function-oriented synthesis studies of the structurally complex marine natural product bryostatin 1[16]. Here we report our efforts to engineer simplified analogues of iboga alkaloids (ibogalogs) that lack the toxicity and hallucinogenic effects of ibogaine but maintain its behavioural effects in rodent models of drug self-administration and relapse.

Function-oriented synthesis of ibogalogs

Characteristic structural features of ibogaine include an indole, a 7-membered tetrahydroazepine and a bicyclic isoquinuclidine (Fig. 1). We reasoned that systematic deletion of these key structural elements would reveal the essential features of the psychoplastogenic pharmacophore of ibogaine. By adapting previously developed chemistry[17], we were able to access a series of isoquinuclidine-containing compounds (**8**–**11**) that lacked the tetrahydroazepine and/or indole moieties that are characteristic of ibogaine (Extended Data Fig. 1a). Ibogalog **8a** lacks both the indole and the tetrahydroazepine rings of ibogaine, whereas **9a**–**11a** lack only the tetrahydroazepine. Ibogamine, ibogaine and noribogaine differ from **9a**, **10a** and **11a** only by the presence of the C2–C16 bond (using the LeMen and Taylor conventions for atom numbering), respectively.

Psychoplastogenic pharmacophore of ibogaine

Except for **11a**, ibogalogs containing the isoquinuclidine but lacking the tetrahydroazepine ring (**8**–**10** and **11b**) were either weak psychoplastogens or did not promote neuronal growth compared to the vehicle control (Extended Data Fig. 2). By contrast, the majority of ibogalogs lacking the isoquinuclidine but retaining the tetrahydroazepine (**12**–**16**) were efficacious (Extended Data Fig. 2). Substitution at C5 of the indole with either fluorine (**15**) or chlorine (**16**) was tolerated, but a more sterically demanding bromine substituent (**17**) in this position was not. We found that ibogainalog (IBG; **13**) showed comparable psychoplastogenic performance to ibogaine despite its simplified chemical structure. We therefore prioritized IBG for further development, because we reasoned that its reduced lipophilicity (calculated logarithm of partition coefficient, clog*P* = 2.61) relative to that of ibogaine (clog*P* = 4.27) would make formulation less challenging and would also reduce the potential for cardiotoxicity, as lipophilicity is a known contributing factor to hERG channel inhibition. The attractiveness of IBG as a potential therapeutic was underscored by its improved central nervous system (CNS) multiparameter optimization (MPO) score[18] (MPO IBG = 5.2; MPO ibogaine = 3.8; optimal MPO = 6.0) coupled with the fact that it can be synthesized in a single step.

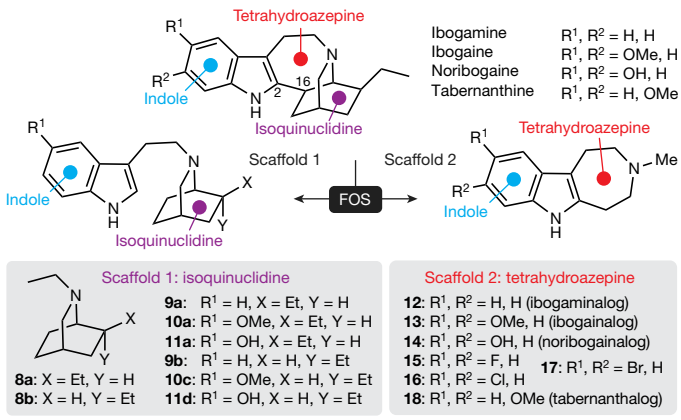

Fig. 1 | Function-oriented synthesis of ibogalogs. The key structural features of ibogaine, related alkaloids and ibogalogs.

TBG is a safer, non-hallucinogenic 5-HT$_{2A}$ agonist

The structure of IBG is similar to that of the potent hallucinogen and serotonin 2A receptor (5-HT$_{2A}$) agonist 5-methoxy-*N*,*N*-dimethyltryptamine (5-MeO-DMT). Previous structure–activity relationship studies demonstrated that, unlike 5-MeO-DMT and other known hallucinogens, 6-MeO-DMT did not substitute for the hallucinogen 2,5-dimethoxy-4-methylamphetamine at any dose in rodents that were trained to discriminate this compound from saline[19]. Moreover, our group has previously shown that 6-MeO-DMT does not produce a head-twitch response[20]—a well-established rodent behavioural proxy for hallucinations induced by 5-HT$_{2A}$ agonists[21]. We therefore synthesized the 6-methoxyindole-fused tetrahydroazepine **18**. Because **18** resembles the iboga alkaloid tabernanthine, we refer to this compound as tabernanthalog (TBG). Like IBG, TBG can be synthesized in a single step, enabling large quantities (more than 1 g) to be rapidly produced.

To evaluate the hallucinogenic potential of IBG and TBG, we tested them in the head-twitch response assay using 5-MeO-DMT (10 mg kg^{-1}) as a positive control (Fig. 2a). Whereas 5-MeO-DMT produces a robust head-twitch response, its conformationally restricted analogue IBG exhibits significantly reduced hallucinogenic potential. As hypothesized, the 6-methoxy substituent of TBG rendered it devoid of hallucinogenic potential as measured by this assay. For these in vivo studies, we used the fumarate salts of IBG and TBG; unlike ibogaine hydrochloride, they are readily soluble in 0.9% saline at concentrations of up to 40 mg ml^{-1} (Extended Data Table 1).

The lipophilicity of ibogaine not only poses practical issues for its administration, but is also likely to be a major contributory factor to its toxicity and adverse cardiac effects. Ibogaine inhibits hERG channels with a half-maximal inhibitory concentration (IC$_{50}$) of 1 μM (Fig. 2b). By contrast, IBG and TBG are approximately 10- and 100-fold less potent than ibogaine, respectively, indicating a lower potential for cardiotoxicity. Administration of ibogaine to immobilized larval zebrafish decreased heart rate (Extended Data Fig. 3a, Supplementary Video 1) and increased the likelihood of inducing arrhythmias, as measured by the ratio of atrial to ventricular beats per minute (Fig. 2c). Neither IBG nor TBG induced these undesirable phenotypes.

To compare the acute behavioural effects of ibogaine, IBG and TBG, we treated larval zebrafish with these compounds across a range of doses (1–200 μM), recorded their behavioural responses to a series of light and acoustic stimuli[20,22] and analysed the resulting behavioural profiles (Extended Data Fig. 3b). Treatment with ibogaine and noribogaine produced behavioural profiles similar to that of the lethal control (Extended Data Fig. 3b, c); by contrast, treatment with IBG and TBG produced behavioural profiles more similar to that of the vehicle control. Zebrafish treated with increasing concentrations of ibogaine, noribogaine and the hERG inhibitors haloperidol, sertindole and terfenadine become more phenotypically distinct from the vehicle control, while more closely resembling the lethal control (eugenol, 100 μM) (Extended Data Fig. 3d). By contrast, treatment with IBG and TBG did not produce this phenotype.

It is currently unclear whether or not ibogaine causes seizures at very high doses[1,23]. We therefore used larval zebrafish expressing GCaMP5

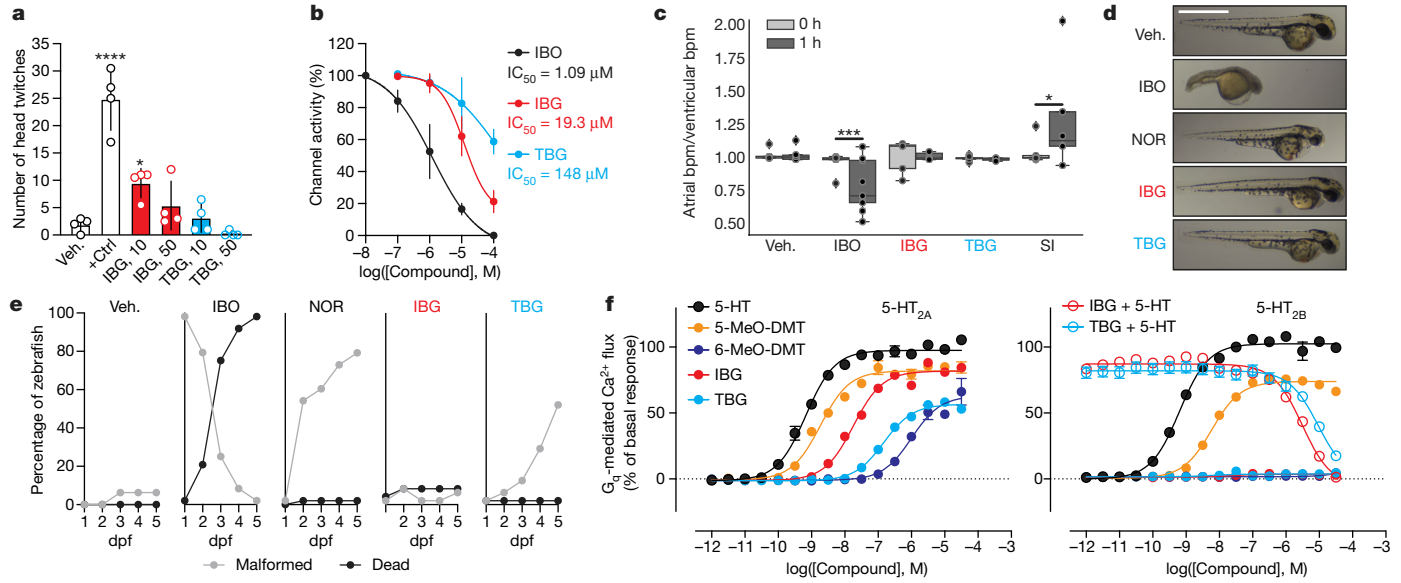

Fig. 2 | TBG is a safer analogue of iboga alkaloids. a, Mouse head-twitch response assays demonstrate that TBG is not hallucinogenic. The doses (mg kg^{-1}) of IBG and TBG are indicated. The positive control (+Ctrl) is 5-MeO-DMT (10 mg kg^{-1}). Veh., vehicle. **b**, Inhibition of hERG channels expressed in HEK293 cells. Data are mean ± s.d. IBO, ibogaine. **c**, Unlike ibogaine, IBG and TBG do not increase the risk of arrhythmias in larval zebrafish. Sertindole (SI) was used as a positive control. bpm, beats per minute. **d**, Representative images of zebrafish treated with compounds (100 µM) for 2 dpf. NOR, noribogaine. Scale bar, 1 mm. **e**, Compound-induced malformations and death over time ($n = 48$ zebrafish for all treatment groups). **f**, Activities at 5-HT_{2A} (left) and 5-HT_{2B} (right) receptors as measured by G_q-mediated calcium flux. Data show the calcium flux response as a percentage of the serotonin-induced maximal response. Exact n values for each experimental condition are reported in the Source Data and in Supplementary Table 1. *$P < 0.05$, ***$P < 0.001$, ****$P < 0.0001$; specific statistical tests, information on reproducibility, and exact P values are reported in Methods and in Supplementary Table 1.

to assess the seizurogenic potential of ibogaine and TBG. Unlike the known seizure-inducing compound pentylenetetrazole, we found that treatment with ibogaine and TBG did not induce excessive neural activity (Extended Data Fig. 3e, Supplementary Video 2).

Finally, we compared the morphological effects of ibogaine, IBG and TBG using a well-established zebrafish developmental toxicity assay[24]. Ibogaine (100 µM) significantly increased malformations and mortality at 2 and 5 days post-fertilization (dpf), respectively (Fig. 2d, e). At both time points, the proportion of viable to non-viable fish was significantly different from that in the vehicle-treated control group ($P < 0.0001$). Ibogaine-treated zebrafish suffered from numerous malformations. Treatment with noribogaine resulted in greater survival, but the majority of zebrafish exhibited yolk sac and/or pericardial oedemas. By contrast, both IBG and TBG treatment (100 µM) resulted in significantly fewer non-viable fish than ibogaine treatment ($P < 0.0001$ for ibogaine versus IBG treatment and ibogaine versus TBG treatment at both 2 and 5 dpf). Notably, reducing the concentration of TBG from 100 to 66 µM resulted in a proportion of viable to non-viable fish that was statistically indistinguishable from that of the vehicle control after 5 dpf ($P = 0.3864$, Extended Data Fig. 3f).

To validate the targets of IBG and TBG, we performed a panel of serotonin (5-HT) and opioid receptor functional assays to assess canonical GPCR signalling. Unlike noribogaine, IBG and TBG showed weak or no opioid agonist activity (Extended Data Figs. 4, 5). However, IBG and TBG demonstrated potent agonist activity at human (Fig. 2f) and mouse (Extended Data Fig. 4) 5-HT_{2A} receptors. Many 5-HT_{2A} agonists—such as 5-MeO-DMT—are also agonists of 5-HT_{2B} receptors, which can lead to cardiac valvulopathy[25]. By contrast, IBG and TBG act as antagonists at 5-HT_{2B} receptors (Fig. 2f). When profiled across the 5-HT receptorome, both IBG and TBG displayed more selective, and potentially safer, profiles as compared to the less conformationally restricted 5-MeO-DMT (Extended Data Figs. 4, 5). A full safety screen across 81 potential targets revealed that TBG exhibits high selectivity for 5-HT_2 receptors (Extended Data Table 2).

To determine whether TBG has rewarding effects, we performed a conditioned place preference assay in mice (Extended Data Fig. 6). A low dose of TBG (1 mg kg^{-1}) did not have any effect on place preference ($P = 0.8972$, comparing pre- and post-conditioning). Higher doses produced a modest conditioned place aversion ($P = 0.0199$ for 10 mg kg^{-1}; $P = 0.0489$ for 50 mg kg^{-1}), which suggests that TBG has a low potential for abuse.

Effect of TBG on neural plasticity

Having demonstrated the improved safety profile of TBG relative to that of ibogaine, we next assessed its effects on structural plasticity. Treatment of rat embryonic cortical neurons with TBG increased dendritic arbor complexity, as measured by Sholl analysis (Fig. 3a); this effect seems to be dependent on the 5-HT_{2A} receptor, as it was blocked by pretreatment with the 5-HT_{2A} antagonist ketanserin (Fig. 3b).

In addition to promoting dendritic growth, TBG also increases dendritic spine density—to an extent comparable to that of ibogaine—in mature (20 days in vitro, DIV20) cortical cultures (Fig. 3c, d). Next, we used transcranial two-photon imaging (Fig. 3e) to assess the effects of TBG on spine dynamics in the mouse sensory cortex. An increase in spine formation, with no effect on spine elimination, was observed 24 hours after treatment with either TBG or the hallucinogenic 5-HT_{2A} agonist 2,5-dimethoxy-4-iodoamphetamine (DOI) (Fig. 3f, g). Similar results were observed in more anterior parts of the cortex, and were consistent with the previously reported effects of ketamine[26].

Effect of TBG on forced swim test behaviour

Increased structural plasticity in the anterior parts of the brain (for example, the prefrontal cortex) have been shown to mediate the sustained (more than 24 h) antidepressant-like effects of ketamine[27] in rodent models and are suggested to have a key role in the therapeutic effects of 5-HT_{2A} agonists[14,28]. We therefore

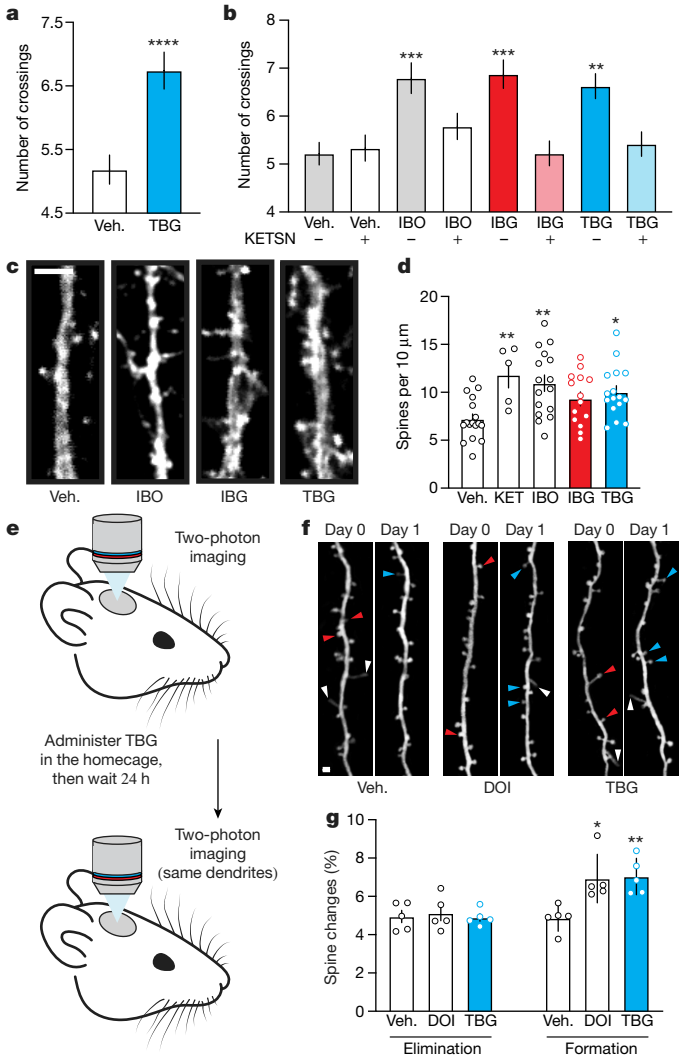

Fig. 3 | TBG promotes neural plasticity. a, Maximum numbers of crossings (N_{max}) of Sholl plots obtained from rat embryonic cortical neurons (DIV6). **b**, The effects of TBG on dendritic growth are blocked by the 5-HT_{2A} antagonist ketanserin (KETSN). **c**, Representative images of secondary branches of rat embryonic cortical neurons (DIV20) after treatment with ibogaine, IBG and TBG for 24 h. Scale bar, 2 µm. **d**, TBG increases dendritic spine density on rat embryonic cortical neurons (DIV20) after treatment for 24 h. KET, ketamine. **e**, Schematic of the design of transcranial two-photon imaging experiments. **f**, Representative images of the same dendritic segments from the mouse primary sensory cortex before (day 0) and after (day 1) treatment. Blue, red and white arrowheads represent newly formed spines, eliminated spines and filopodia, respectively. Scale bar, 2 µm. **g**, 2,5-Dimethoxy-4-iodoamphetamine (DOI) and TBG increase spine formation but have no effect on spine elimination. Exact *n* values for each experimental condition are reported in the Source Data and in Supplementary Table 1. $^{*}P < 0.05$, $^{**}P < 0.01$, $^{***}P < 0.001$, $^{****}P < 0.0001$; specific statistical tests, information on reproducibility, and exact *P* values are reported in Methods and in Supplementary Table 1.

evaluated the effect of TBG on the behaviour of mice in a forced swim test after 7 days of unpredictable mild stress (Extended Data Fig. 7a, b). The amount of time spent immobile was significantly increased after stress. This effect was rescued by a 50 mg kg^{-1}, but not a 10 mg kg^{-1}, dose of TBG. Preliminary pharmacokinetic studies revealed that a 50 mg kg^{-1} dose of TBG produced significantly higher concentrations in the brain than did a 10 mg kg^{-1} dose (Extended Data Fig. 7c). Therefore, the 50 mg kg^{-1} dose was used in subsequent mouse behavioural experiments.

Because ketamine produces antidepressant-like effects in the forced swim test even in the absence of unpredictable mild stress, we performed a direct comparison of the effects of ketamine and TBG (Fig. 4a, b). Drugs were administered 24 h after a pre-test, and the forced swim test was then performed 24 h and 7 d after drug administration. Both ketamine and TBG significantly reduced immobility in mice 24 h after drug administration; however, the effects of ketamine seemed to be more durable. Notably, TBG had no effect on locomotion 24 h after administration (Extended Data Fig. 6c). As anticipated, treatment with a 5-HT_{2A} antagonist, ketanserin, blocked the antidepressant-like effect of TBG (Fig. 4b). The efficacy exhibited by TBG in the forced swim test is consistent with the fact that other 5-HT_{2A} agonists have demonstrated potential for the treatment of depression[13,28]. However, future studies should evaluate the effects of TBG on other behaviours that are relevant to depression, particularly those that measure anhedonia.

TBG reduces alcohol- and heroin-seeking behaviour

To assess the effect of TBG on alcohol (ethanol) intake, we used an intermittent-access, two-bottle choice experiment (20% ethanol (v/v) versus water) that models binge-drinking behaviour in humans[29]. Mice underwent repeated cycles of binge drinking and withdrawal over the course of 7 weeks (Fig. 4c), which resulted in high ethanol consumption (11.44 ± 0.76 g per kg per 24 h) and binge-drinking-like behaviour (3.89 ± 0.33 g per kg per 4 h) and generated a blood-alcohol content equivalent to that of humans with alcohol use disorder. Systemic injections of TBG 3 hours before a drinking session reduced binge drinking during the first 4 hours of the session without affecting water intake (Fig. 4d). Alcohol consumption was lower for at least 2 days after TBG administration (Fig. 4e). Similar results have been observed previously for ibogaine[3]. Notably, administration of TBG before giving mice access to both water and a 5% sucrose solution did not decrease sucrose preference (Fig. 4f) or total fluid consumption (Fig. 4g), indicating that TBG selectively reduced alcohol intake.

As with alcohol consumption, there are anecdotal reports to suggest that ibogaine can reduce opioid use in humans[1,6]. In rodent models of opioid self-administration[30], the greatest decrease is seen when ibogaine is administered at a dose of 40 mg kg^{-1}. Here, we used a rat model of heroin self-administration (Fig. 4h) to assess the effects of TBG (40 mg kg^{-1}) administered during three distinct periods: during self-administration, before the first day of extinction, and immediately before cued reinstatement. As a control, vehicle was administered at these same time points whenever TBG was not (Fig. 4i); each group therefore received a total of three injections. When administered during self-administration (Fig. 4j, k), immediately before extinction (Fig. 4l) or before cued reinstatement (Fig. 4m), TBG acutely reduced heroin-seeking behaviour. Although TBG did not induce any acute locomotor deficits (Extended Data Fig. 8a), the acute effects of TBG should be interpreted with caution. Similar to heroin, acute TBG administration strongly reduced sucrose self-administration at all three time points (Extended Data Fig. 8b–e), indicating that the acute effects of TBG may be due to non-selective disruption of operant responding.

Notably, cue-induced relapse was reduced in the groups that were treated with TBG long before cued reinstatement (that is, during self-administration and before the first day of extinction; Fig. 4m). By contrast, TBG had no effect on cued reinstatement of sucrose-seeking behaviour when it was administered 12–14 days previously (Extended Data Fig. 8e). Therefore, a single administration of TBG elicited anti-addictive effects lasting up to 12–14 days. Long-lasting protection against relapse after a single treatment has rarely been reported, but is reminiscent of results in a cocaine self-administration model after the direct injection of brain-derived neurotrophic factor into the prefrontal cortex[31].

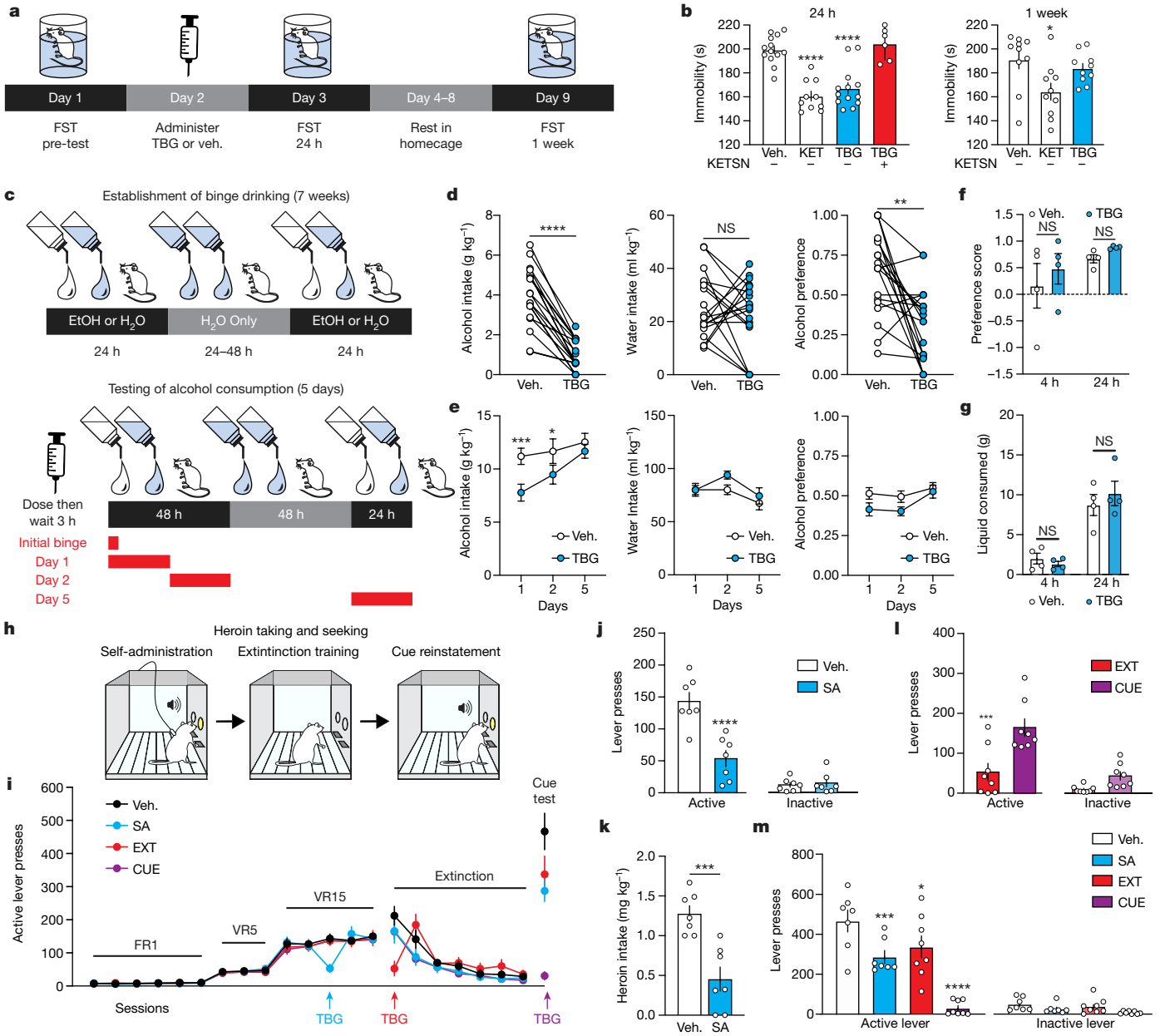

Fig. 4 | Effects of TBG on animal behaviours relevant to depression, alcohol use disorder and substance use disorder. a, Schematic of the design of forced swim test (FST) experiments conducted without unpredictable mild stress. **b**, The antidepressant-like effects of TBG are blocked by ketanserin. **c**, Timeline of alcohol binge-drinking experiment. White and blue droplets represent 20% ethanol (EtOH) and H_2O, respectively. **d**, TBG acutely reduced ethanol consumption and preference during a binge-drinking session without affecting H_2O intake. **e**, Acute TBG administration decreased ethanol consumption for at least 48 h. **f**, **g**, TBG did not decrease sucrose preference (**f**) or reduce total liquid consumption (**g**) in a two-bottle choice experiment. **h**, Schematic of the design of the heroin self-administration experiments. **i**, Heroin seeking over time. Coloured arrows indicate when each group received TBG. Vehicle was administered at all other time points to each group. SA, self-administration; EXT, extinction; CUE, cued reinstatement; FR1, fixed ratio 1; VR5, variable ratio 5; VR15, variable ratio 15. **j**, **k**, TBG acutely reduced heroin self-administration—both lever pressing (**j**) and heroin intake (**k**). **l**, TBG acutely reduced heroin-seeking when administered immediately before the first extinction session. The cued reinstatement (injection 1, vehicle; injection 2, vehicle) and extinction (injection 1, vehicle; injection 2, TBG) groups were compared, as they were matched for the number of withdrawal days between the last self-administration and first extinction session. **m**, Acute TBG administration completely blocked cued reinstatement (purple bar). A single previous (12–14 d) administration of TBG during heroin self-administration or on the first day of extinction (blue and red bars, respectively) inhibited cued reinstatement. Exact *n* values for each experimental condition are reported in the Source Data and in Supplementary Table 1. *$P < 0.05$, **$P < 0.01$, ***$P < 0.001$, ****$P < 0.0001$; specific statistical tests, information on reproducibility, and exact *P* values are reported in Methods and in Supplementary Table 1.

Discussion

Compounds that are capable of modifying neural circuits that control motivation, anxiety and drug-seeking behaviour have been proposed to be effective treatments for a diverse range of neuropsychiatric disorders including depression, post-traumatic stress disorder and substance use disorder[13]. In principle, such psychoplastogenic medicines could produce sustained therapeutic effects by rectifying underlying pathological changes in circuitry rather than by masking symptoms of the disorder. Psychedelic compounds could prove useful in this regard

because they promote structural and functional neural plasticity in the prefrontal cortex of rodents[14]. Although their putative therapeutic mechanisms of action are unknown, anecdotal reports and small clinical trials suggest that they might produce sustained therapeutic responses in several neuropsychiatric disorders after a single administration.

It has been suggested that psychedelic compounds and ketamine share a common antidepressant mechanism of action that is related to cortical neuron growth in the prefrontal cortex; however, a causal link between psychedelic-induced neuronal growth and behaviour has yet to be established in either humans or rodents. By contrast, a synapse-targeting photoactivatable RAC1 has recently been used to demonstrate that the sustained antidepressant-like effects of ketamine in mice are mediated in part by spinogenesis in the prefrontal cortex[27].

Here we used the principles of function-oriented synthesis to identify the indole-fused tetrahydroazepine as the key psychoplastogenic pharmacophore of ibogaine. This information enabled us to develop a one-step synthesis of ibogaine analogues that are capable of promoting structural neural plasticity both in cell culture and in vivo. Simplification of the architecture of ibogaine to produce TBG not only enhanced synthetic tractability but also improved physicochemical properties and safety. Compounds lacking the isoquinuclidine moiety were significantly less potent inhibitors of hERG channels and did not induce bradycardia or show signs of toxicity in zebrafish. With the exception of 18-methoxycoronaridine (18-MC), which is currently in phase II clinical trials, very few ibogaine analogues have demonstrated this level of safety while also producing therapeutic effects[32]. It is not known if 18-MC is psychoplastogenic; however, unlike ibogaine, it does not increase the expression of *GDNF* in SH-SY5Y cells or reduce alcohol self-administration after direct infusion into the ventral tegmental area, which suggests that their mechanisms of action are probably distinct[33]. In addition, whereas the synthesis of 18-MC requires 13 steps[34], TBG can be synthesized in a single step.

Not only does TBG potently promote neuronal growth, it also produces antidepressant-like behavioural responses and reduces alcohol—but not sucrose—consumption in mice. In rats, acute administration of TBG strongly inhibits both heroin- and sucrose-seeking behaviour, probably by disrupting operant responding. However, when administered days in advance, TBG prevents only cued reinstatement of heroin-seeking behaviour and not sucrose-seeking behaviour. Future work is required to further characterize the optimal dosing regimen and time course to produce these behavioural effects in rodents, and to determine whether structural plasticity has a causal role.

Online content

Any methods, additional references, Nature Research reporting summaries, source data, extended data, supplementary information, acknowledgements, peer review information; details of author contributions and competing interests; and statements of data and code availability are available at https://doi.org/10.1038/s41586-020-3008-z.

1. Wasko, M. J., Witt-Enderby, P. A. & Surratt, C. K. DARK classics in chemical neuroscience: ibogaine. *ACS Chem. Neurosci.* **9**, 2475–2483 (2018).
2. Noller, G. E., Frampton, C. M. & Yazar-Klosinski, B. Ibogaine treatment outcomes for opioid dependence from a twelve-month follow-up observational study. *Am. J. Drug Alcohol Abuse* **44**, 37–46 (2018).
3. He, D. Y. et al. Glial cell line-derived neurotrophic factor mediates the desirable actions of the anti-addiction drug ibogaine against alcohol consumption. *J. Neurosci.* **25**, 619–628 (2005).
4. Marton, S. et al. Ibogaine administration modifies GDNF and BDNF expression in brain regions involved in mesocorticolimbic and nigral dopaminergic circuits. *Front. Pharmacol.* **10**, 193 (2019).
5. Jenks, C. W. Extraction studies of *Tabernanthe iboga* and *Voacanga africana*. *Nat. Prod. Lett.* **16**, 71–76 (2002).
6. Iyer, R. N., Favela, D., Zhang, G. & Olson, D. E. The iboga enigma: the chemistry and neuropharmacology of iboga alkaloids and related analogs. *Nat. Prod. Rep.* https://doi.org/10.1039/D0NP00033G (2020).
7. Hough, L. B., Pearl, S. M. & Glick, S. D. Tissue distribution of ibogaine after intraperitoneal and subcutaneous administration. *Life Sci.* **58**, PL119–PL122 (1996).
8. Koenig, X., Kovar, M., Boehm, S., Sandtner, W. & Hilber, K. Anti-addiction drug ibogaine inhibits hERG channels: a cardiac arrhythmia risk. *Addict. Biol.* **19**, 237–239 (2014).
9. Thurner, P. et al. Mechanism of hERG channel block by the psychoactive indole alkaloid ibogaine. *J. Pharmacol. Exp. Ther.* **348**, 346–358 (2014).
10. Alper, K. R., Stajić, M. & Gill, J. R. Fatalities temporally associated with the ingestion of ibogaine. *J. Forensic Sci.* **57**, 398–412 (2012).
11. Koenig, X. & Hilber, K. The anti-addiction drug ibogaine and the heart: a delicate relation. *Molecules* **20**, 2208–2228 (2015).
12. Baumann, M. H., Pablo, J. P., Ali, S. F., Rothman, R. B. & Mash, D. C. Noribogaine (12-hydroxyibogamine): a biologically active metabolite of the antiaddictive drug ibogaine. *Ann. NY Acad. Sci.* **914**, 354–368 (2000).
13. Olson, D. E. Psychoplastogens: a promising class of plasticity-promoting neurotherapeutics. *J. Exp. Neurosci.* **12**, 1179069518800508 (2018).
14. Ly, C. et al. Psychedelics promote structural and functional neural plasticity. *Cell Rep.* **23**, 3170–3182 (2018).
15. Bogenschutz, M. P. & Johnson, M. W. Classic hallucinogens in the treatment of addictions. *Prog. Neuropsychopharmacol. Biol. Psychiatry* **64**, 250–258 (2016).
16. Wender, P. A., Verma, V. A., Paxton, T. J. & Pillow, T. H. Function-oriented synthesis, step economy, and drug design. *Acc. Chem. Res.* **41**, 40–49 (2008).
17. Gassaway, M. M. et al. Deconstructing the iboga alkaloid skeleton: potentiation of FGF2-induced glial cell line-derived neurotrophic factor release by a novel compound. *ACS Chem. Biol.* **11**, 77–87 (2016).
18. Wager, T. T., Hou, X., Verhoest, P. R. & Villalobos, A. Central nervous system multiparameter optimization desirability: application in drug discovery. *ACS Chem. Neurosci.* **7**, 767–775 (2016).
19. Glennon, R. A., Young, R., Jacyno, J. M., Slusher, M. & Rosecrans, J. A. DOM-stimulus generalization to LSD and other hallucinogenic indolealkylamines. *Eur. J. Pharmacol.* **86**, 453–459 (1983).
20. Dunlap, L. E. et al. Identification of psychoplastogenic *N*,*N*-dimethylaminoisotryptamine (isoDMT) analogs through structure–activity relationship studies. *J. Med. Chem.* **63**, 1142–1155 (2020).
21. Halberstadt, A. L., Chatha, M., Klein, A. K., Wallach, J. & Brandt, S. D. Correlation between the potency of hallucinogens in the mouse head-twitch response assay and their behavioral and subjective effects in other species. *Neuropharmacology* **167**, 107933 (2020).
22. McCarroll, M. N. et al. Zebrafish behavioural profiling identifies GABA and serotonin receptor ligands related to sedation and paradoxical excitation. *Nat. Commun.* **10**, 4078 (2019).
23. Breuer, L. et al. "Herbal seizures" – atypical symptoms after ibogaine intoxication: a case report. *J. Med. Case Rep.* **9**, 243 (2015).
24. Dach, K. et al. Teratological and behavioral screening of the national toxicology program 91-compound library in zebrafish (*Danio rerio*). *Toxicol. Sci.* **167**, 77–91 (2019).
25. Rothman, R. B. & Baumann, M. H. Serotonergic drugs and valvular heart disease. *Expert Opin. Drug Saf.* **8**, 317–329 (2009).
26. Phoumthipphavong, V., Barthas, F., Hassett, S., Kwan, A. C. Longitudinal effects of ketamine on dendritic architecture in vivo in the mouse medial frontal cortex. *eNeuro* **3**, 0133-15 (2016).
27. Moda-Sava, R. N. et al. Sustained rescue of prefrontal circuit dysfunction by antidepressant-induced spine formation. *Science* **364**, eaat8078 (2019).
28. Cameron, L. P. & Olson, D. E. Dark classics in chemical neuroscience: *N*,*N*-dimethyltryptamine (DMT). *ACS Chem. Neurosci.* **9**, 2344–2357 (2018).
29. Warnault, V., Darcq, E., Levine, A., Barak, S. & Ron, D. Chromatin remodelling — a novel strategy to control excessive alcohol drinking. *Transl. Psychiatry* **3**, e231 (2013).
30. Glick, S. D. et al. Effects of iboga alkaloids on morphine and cocaine self-administration in rats: relationship to tremorigenic effects and to effects on dopamine release in nucleus accumbens and striatum. *Brain Res.* **657**, 14–22 (1994).
31. Giannotti, G., Barry, S. M., Siemsen, B. M., Peters, J. & McGinty, J. F. Divergent prelimbic cortical pathways interact with BDNF to regulate cocaine-seeking. *J. Neurosci.* **38**, 8956–8966 (2018).
32. Glick, S. D., Kuehne, M. E., Maisonneuve, I. M., Bandarage, U. K. & Molinari, H. H. 18-Methoxycoronaridine, a non-toxic iboga alkaloid congener: effects on morphine and cocaine self-administration and on mesolimbic dopamine release in rats. *Brain Res.* **719**, 29–35 (1996).
33. Carnicella, S., He, D. Y., Yowell, Q. V., Glick, S. D. & Ron, D. Noribogaine, but not 18-MC, exhibits similar actions as ibogaine on GDNF expression and ethanol self-administration. *Addict. Biol.* **15**, 424–433 (2010).
34. Bandarage, U. K., Kuehne, M. E. & Glick, S. D. Total syntheses of racemic albifloranine and its anti-addictive congeners, including 18-methoxycoronaridine. *Tetrahedron* **55**, 9405–9424 (1999).

Publisher's note Springer Nature remains neutral with regard to jurisdictional claims in published maps and institutional affiliations.

© The Author(s), under exclusive licence to Springer Nature Limited 2020

Methods

Data analysis and statistics

Treatments were randomized, and data were analysed by experimenters blinded to treatment conditions. Statistical analyses were performed using GraphPad Prism (v.8.1.2) unless noted otherwise. All comparisons were planned before performing each experiment. Statistical methods were not used to predetermine sample sizes, with the exception that power analyses were conducted to estimate animal numbers for in vivo experiments. Data are represented as mean ± s.e.m., unless otherwise noted, with asterisks indicating $^{*}P < 0.05$, $^{**}P < 0.01$, $^{***}P < 0.001$ and $^{****}P < 0.0001$. Box plots depict the three quartile values of the distribution with whiskers extending to points that lie within 1.5 IQRs (interquartile range) of the lower and upper quartile. Observations falling outside this range are displayed independently. For Figs. 2a, 3a, b, d, g, 4b, Extended Data Fig. 2b and Extended Data Fig. 7b, compound treatments were compared to the vehicle control using a one-way ANOVA with Dunnett's post hoc test. For Extended Data Fig. 3a and Fig. 2c, time 0 h and time 1 h (before and after drug administration, respectively) data were compared using a paired *t*-test. For Fig. 2e and Extended Data Fig. 3f, compound treatments were compared using Fisher's exact test and *P* values are indicated in the text. For Fig. 4d and Extended Data Fig. 6b, data were analysed using a two-tailed paired *t*-test. Data in Fig. 4e–g and Extended Data Fig. 8a (distance and velocity) were analysed using a two-way ANOVA with Sidak's post hoc test. For Fig. 4j, l–m and Extended Data Fig. 8c–e, two-way repeated measures (RM) ANOVAs with treatment group as the between-subject factor and lever type (active versus inactive) as the within-subject factor were used. Sidak post hoc tests were conducted as appropriate. For Extended Data Fig. 6c, a one-way ANOVA with Tukey's post hoc test was used. For Fig. 4k and Extended Data Fig. 8a (thigmotaxis) two-tailed unpaired *t*-tests were used.

Drugs

The NIDA Drug Supply Program provided ibogaine hydrochloride, noribogaine, heroin (diamorphine hydrochloride) and cocaine hydrochloride. Other chemicals were purchased from commercial sources as follows: ketamine hydrochloride (Fagron), ketanserin (ApexBio), eugenol (Tokyo Chemical Industries) and 5-hydroxytryptamine (Sigma-Aldrich). The fumarate salt of 5-methoxy-*N*,*N*-dimethyltryptamine (2:1, 5-MeO-DMT:fumaric acid) was synthesized in-house as described previously[20] and judged to be analytically pure on the basis of nuclear magnetic resonance (NMR) and liquid chromatography–mass spectrometry (LC–MS) data. For cell culture experiments, the vehicle was a 0.1% (agonist studies) or 0.2% (antagonist studies) molecular biology grade dimethyl sulfoxide (DMSO) (Sigma-Aldrich) solution. For in vivo experiments, the vehicle was USP grade saline (0.9%). Free bases were used for all cellular experiments and the fumarate salts of ibogainalog and tabernanthalog were used for the in vivo studies.

Animals

All experimental procedures involving animals were approved by either the University of California, Davis (UCD), the University of California, San Francisco (UCSF), the University of California, Santa Cruz (UCSC), or the University of Colorado Denver, Anschutz Medical Campus (CU Anschutz) Institutional Animal Care and Use Committee (IACUC) and adhered to principles described in the National Institutes of Health Guide for the Care and Use of Laboratory Animals. Power analyses were conducted to ensure appropriate sample size for all experiments involving animals. UCD, UCSF, UCSC and CU Anschutz are accredited by the Association for Assessment and Accreditation of Laboratory Animal Care International (AAALAC).

Calculation of CNS MPO score

CNS MPO scores were calculated using a previously published method[18]. Predicted pK_a values were determined using Marvin Sketch (19.25.0). log*P* and total polar surface area were predicted using Molinspiration (https://www.molinspiration.com/). log*D* (the logarithm of the distribution coefficient) was calculated using the following equation $\log D = \log P - \log_{10}(1 + 10^{(pKa - 7.4)})$.

Dendritogenesis experiments

For the dendritogenesis experiments conducted using cultured cortical neurons, timed pregnant Sprague Dawley rats were obtained from Charles River Laboratories. Full culturing, staining and analysis experiments were performed as previously described[20]. Dendrites were visualized using a chicken anti-MAP2 antibody (1:10,000; EnCor, CPCA-MAP2) as previously reported[20].

Head-twitch response

The head-twitch response assay was performed as described previously[20] using both male and female C57BL/6J mice (2 each per treatment). The mice were obtained from Jackson Laboratory and were approximately 8 weeks old at the time of the experiments. Compounds were administered via intraperitoneal (i.p.) injection (5 ml kg^{-1}) using 0.9% saline as the vehicle. As a positive control, we used 5-MeO-DMT fumarate (2:1 amine/acid), which was synthesized as described previously[20]. Behaviour was videotaped, later scored by two blinded observers, and the results were averaged (Pearson correlation coefficient = 0.93).

hERG inhibition studies

All experiments were conducted manually using a HEKA EPC-10 amplifier at room temperature in the whole-cell mode of the patch-clamp technique. HEK293 cells stably expressing hKv11.1 (hERG) under G418 selection were a gift from C. January (University of Wisconsin, Madison). Cells were cultured in DMEM containing 10% fetal bovine serum, 2 mM glutamine, 1 mM sodium pyruvate, 100 U ml^{-1} penicillin, 100 μg ml^{-1} streptomycin, and 500 mg ml^{-1} G418. The cell line was not authenticated or tested for mycoplasma contamination. Before experiments, cells were grown to 60–80% confluency, lifted using TrypLE, and plated onto poly-L-lysine-coated coverslips. Patch pipettes were pulled from soda lime glass (micro-haematocrit tubes) and had resistances of 2–4 MΩ. For the external solution, normal sodium Ringer was used (160 mM NaCl, 4.5 mM KCl, 2 mM $CaCl_2$, 1 mM $MgCl_2$, 10 mM HEPES, pH 7.4 and 290–310 mOsm). The internal solution used was potassium fluoride with ATP (160 mM KF, 2 mM $MgCl_2$, 10 mM EGTA, 10 mM HEPES, 4 mM NaATP, pH = 7.2 and 300–320 mOsm). A two-step pulse (applied every 10 s) from −80 mV initially to 40 mV for 2 s and then to −60 mV for 4 s, was used to elicit hERG currents. The percentage reduction of tail current amplitude by the drugs was determined and data are shown as mean ± s.d. (n = 3–4 per data point). For all experiments, solutions of the drugs were prepared fresh from 10 mM stocks in DMSO. The final DMSO concentration never exceeded 1%.

Larval zebrafish heart rate experiments

Zebrafish express Zerg, an orthologue of hERG, and many hERG inhibitors induce bradycardia and arrhythmia in zebrafish[35]. Heart rate was recorded and calculated as reported previously[36] with slight modifications (n = 3–9). In brief, 7 dpf zebrafish larvae were anaesthetized with tricaine (Acros Organics) and immobilized in a lateral orientation using 1% low melt agarose (LMA, Gene Mate) dissolved in egg water[37]. Tricaine was washed out and the drug was added to 4 ml embryo media in a 6-well plate (final concentration 50 μM). Videos were collected at 30 frames per second (fps) using a Leica M80 scope with an ACHRO 1× nosepiece attachment and a Leica IC80 HD camera. Regions of interest (ROIs) were drawn around the atrium and ventricle of individual zebrafish and average pixel dynamics were calculated using the ImageJ plugin Time Series Analyzer V3. This pixel change oscillation was graphically smoothed using the Savgol filter in SciPy. Peaks were detected using the SciPy package "find_peaks". Peak time interval and heart rate (bpm)

were calculated using custom code. The arrythmia score was calculated as the ratio of atrial bpm to ventricular bpm ($n = 6–18$).

Larval zebrafish behavioural experiments

Behavioural data were collected and analysed as described previously[20,22], with slight modifications. Locomotion of 7 dpf zebrafish was recorded at 100 fps under a 17-min series of acoustic and light-based stimuli 1 h after treatment. Data were collected in a concentration–response format on eight 96-well plates with 8 zebrafish per well. Each plate contained all 10 compounds at 8 concentrations plus 8 DMSO (vehicle) and 8 eugenol (lethal) control wells. Treatments and well positions were scrambled according to two randomized plate layouts. Motion in Extended Data Fig. 3a was smoothed using the mean over a 10-frame sliding window. Classifiers were trained as previously described[22]. For Extended Data Fig. 3d, 6 repeat vs-solvent and 6 repeat vs-lethal classifiers (3,000 trees) were trained per comparison, each to classify 8 treatment wells and 8 randomly subsampled control wells. Responses were calculated from the out-of-bag accuracy values as $r = (a - 0.4)/(1 - 0.4)$. 95% confidence intervals were calculated over 1,000 bootstrap samples per comparison. For Extended Data Fig. 3b, a single classifier (10,000 trees) was trained on all data for the treatments shown, and the out-of-bag predictions were used.

Larval zebrafish seizure experiments

At 6 dpf, transgenic zebrafish larvae (*Tg(elavl3:GCaMP5G)a4598*)[38] were anaesthetized with tricaine and immobilized in a dorsal orientation using 1% LMA dissolved in egg water. Tricaine was washed out and zebrafish were treated for 1 h with compounds (50 μM for IBO and TBG; 15 mM for pentylenetetrazole (PTZ)). Videos were acquired using a Zeiss Axiozoom.V16, and GCaMP5G fluorescence was induced using a Lumencor sola light engine. Zen software V2 blue edition controlled an Axiocam 506 mono camera set to 33 fps. Short videos (1–3 min) were acquired per condition. Change in fluorescence intensity (F) was calculated using ImageJ from an ROI drawn in the cerebellar region, and $\Delta F/F$ was calculated and visualized using custom functions.

Larval zebrafish toxicity

Tropical 5D wild-type larval zebrafish were obtained from the Sinnhuber Aquatic Research Laboratory (SARL) at Oregon State University, and subsequent generations were raised at UCD. Zebrafish husbandry, spawning, dechorionation of embryos and exposures were performed as described previously[24]. Chemical stocks were prepared at 100 mM in DMSO and diluted to 200 μM with embryo media. This solution was diluted twofold into individual wells of 96-well plates housing larval zebrafish. The final compound and DMSO concentrations were 100 μM and 0.1% (v/v), respectively. Wells were covered with Parafilm M (Bemis) then covered with the plate lid. Plates were maintained in an incubator at 28.5 °C with a 14 h light (~300 lx)/10 h dark cycle. Fish were statically exposed to compounds 6 hours post-fertilization (hpf) through 5 dpf. All compounds were tested for mortality or teratology in triplicate experiments (three experiments conducted on independent days using fish from independent spawns). For each experiment, 16 fish were tested per concentration per compound ($n = 48$ fish per condition). At 1, 2, 3, 4, and 5 dpf, fish were examined for mortality and developmental malformations using a Leica Stereo Microscope Model S6D (Leica) up to 4.5× magnification.

Serotonin and opioid receptor functional assays

Functional assay screens at 5-HT and opioid receptors were performed in parallel using the same compound dilutions and 384-well-format high-throughput assay platforms. Assays assessed activity at all human isoforms of the receptors, except where noted for the mouse 5-HT_{2A} receptor. Receptor constructs in pcDNA vectors were generated from the Presto-Tango GPCR library[39] with minor modifications. All compounds were serially diluted in drug buffer (HBSS, 20 mM HEPES, pH 7.4 supplemented with 0.1% bovine serum albumin and 0.01% ascorbic acid) and dispensed into 384-well assay plates using a FLIPR Tetra automated dispenser head (Molecular Devices). Every plate included a positive control such as 5-HT (for all 5-HT receptors), DADLE (DOR), salvinorin A (KOR), and DAMGO (MOR). For measurements of 5-HT_{2A}, 5-HT_{2B}, and 5-HT_{2C} G_q-mediated calcium flux function, HEK Flp-In 293 T-Rex stable cell lines (Invitrogen) were loaded with Fluo-4 dye for one hour, stimulated with compounds and read for baseline (0–10 s) and peak fold-over-basal fluorescence (5 min) at 25 °C on the FLIPR Tetra system. For measurement of 5-HT_6 and 5-HT_{7a} functional assays, G_s-mediated cAMP accumulation was detected using the split-luciferase GloSensor assay in HEKT cells measuring luminescence on a Microbeta Trilux (Perkin Elmer) with a 15 min drug incubation at 25 °C. For 5-HT_{1A}, 5-HT_{1B}, 5-HT_{1F}, MOR, KOR and DOR functional assays, $G_{i/o}$-mediated cAMP inhibition was measured using the split-luciferase GloSensor assay in HEKT cells, conducted similarly to that above, but in combination with either 0.3 μM isoproterenol (5-HT_{1A}, 5-HT_{1B}, 5-HT_{1F}) or 1 μM forskolin (MOR, KOR and DOR) to stimulate endogenous cAMP accumulation. For measurement of 5-HT_{1D}, 5-HT_{1E}, 5-HT_4, and 5-HT_{5A} functional assays, β-arrestin2 recruitment was measured by the Tango assay using HTLA cells expressing tobacco etch virus (TEV) fused-β-arrestin2, as described previously[39] with minor modifications. Cell lines were not authenticated, but they were purchased mycoplasma-free and tested for mycoplasma contamination. Data for all assays were plotted and nonlinear regression was performed using "log(agonist) vs. response" in GraphPad Prism to yield estimates of the efficacy (E_{max}) and half-maximal effective concentration (EC_{50}).

Safety pharmacology profiling panel

TBG (10 μM) was screened by Eurofins Discovery against their SafetyScreen87 Panel and in their VMAT (non-selective) human vesicular monoamine transporter binding assay.

Conditioned place preference assay

The conditioned place preference apparatus consisted of two chambers (18 cm L × 20 cm W × 35 cm H) connected by a corridor (10 cm L × 20 cm W × 35 cm H). One chamber had a smooth floor and black walls whereas the second chamber had a mesh floor and patterned walls. A block was placed in the corridor to restrict mice to a particular chamber. On day 1 (pre-conditioning), male C57/BL6J mice (9–10 weeks old) were allowed to explore the entire apparatus for 30 min. Mice were randomly sorted into treatment groups (TBG at 50 mg kg^{-1}, 10 mg kg^{-1} and 1 mg kg^{-1}), ensuring that their initial preferences for what would become the TBG-paired side were approximately equal. Next, the mice were administered an i.p. injection of either vehicle (saline) or TBG (counterbalanced) immediately before being confined to one of the two chambers for 30 min. The following day, the other treatment was administered, and the mice were confined to the opposite chamber for 30 min. This sequence was repeated twice, such that all mice received 3 vehicle-side pairings and 3 TBG-side pairings. The mice were returned to their homecages in between treatment-side pairings. On day 8 (post conditioning), the mice were allowed to explore the entire apparatus for 30 min, and the time spent on the vehicle- and TBG-paired sides was quantified using ANYmaze software (v.6.2). The apparatus was cleaned with 70% ethanol between trials. Drug solutions were prepared fresh daily.

Pharmacokinetic studies

Male and female C57/BL6J mice (12 weeks old) were administered TBG via i.p. injection at doses of either 50 mg kg^{-1}, 10 mg kg^{-1} or 1 mg kg^{-1}. Mice were euthanized 15 min or 3 h after injection by cervical dislocation. Two males and two females were used per dose and time point. Brain and liver were collected, flash-frozen in liquid nitrogen, and stored at −80 °C until metabolomic processing. Metabolites were extracted from tissue as described previously[40]. In brief, whole brain and liver

sections were lyophilized overnight to complete dryness, then homogenized with 3.2-mm diameter stainless-steel beads using a GenoGrinder for 50 s at 1,500 rpm. Ground tissue was then extracted using 225 µl cold methanol, 190 µl water, 750 µl methyl *tert*-butyl ether (MTBE). Seven method blanks and seven quality-control samples (pooled human serum, BioIVT) were extracted at the same time as the samples. The nonpolar fraction of MTBE was dried under vacuum and reconstituted in 60 µl of 90:10 (v/v) methanol: toluene containing 1-cyclohexyldodecanoic acid urea as an internal standard. Samples were then vortexed, sonicated and centrifuged before analysis. For analysis of TBG in liver and brain, samples were randomized before injection with method blanks and quality-control samples were analysed between every ten study samples. A six-point calibration curve was analysed after column equilibration using blank injections, and then after all study samples. Blanks were injected after the calibration curve to ensure no that no TBG was retained on the column and carried over to samples. Reconstituted sample (5 µl) was injected onto a Waters Acquity UPLC CSH C18 column (100 mm × 2.1 mm, 1.7 µm particle size) with an Acquity UPLC CSH C18 VanGuard precolumn (Waters) using a Vanquish UHPLC coupled to a TSQ Altis triple quadrupole mass spectrometer (Thermo Fisher Scientific). Mobile phase A consisted of 60:40 v/v acetonitrile/water with 10 mM ammonium formate and 0.1% formic acid. Mobile phase B was 90:10 v/v isopropanol/acetonitrile with 10 mM ammonium formate and 0.1% formic acid. Gradients were run from 0–2 min at 15% B; 2–2.5 min 30% B; 2.5–4.5 min 48% B; 4.5–7.3 min 99% B; 7.3–10 min 15% B. The flow rate was 0.600 ml min^{-1} and the column was heated to 65 °C. Mass spectrometer conditions were optimized for TBG by direct infusion. Selected reaction monitoring was performed for the top five ions, with collision energy, source fragmentation, and radiofrequency optimized for TBG. Data were processed with TraceFinder 4.1 (Thermo Fisher Scientific). Organ weights were recorded. The concentration in the brain was calculated using the experimentally determined number of moles of TBG in the whole organ divided by the weight of the organ.

Spinogenesis experiments

Spinogenesis experiments were performed as previously described[14], with the exception that cells were treated on DIV19 and fixed 24 h after treatment on DIV20. The images were taken on a Nikon HCA Confocal microscope a with a 100×/NA 1.45 oil objective. DMSO and ketamine (10 µM) were used as vehicle and positive controls, respectively.

In vivo spine dynamics

Male and female *Thy1*-GFP-M line mice[41] ($n = 5$ per condition) were purchased from The Jackson Laboratory (JAX 007788) and maintained in the animal facilities at UCSC according to an IACUC-approved protocol. In vivo transcranial two-photon imaging and data analysis were performed as previously described[42]. In brief, mice were anaesthetized with an i.p. injection of a mixture of ketamine (87 mg kg^{-1}) and xylazine (8.7 mg kg^{-1}). A small region of the exposed skull was manually thinned down to 20–30 µm for optical access. Spines on apical dendrites in mouse primary sensory cortices were imaged using a Bruker Ultima IV two-photon microscope equipped with an Olympus water-immersion objective (40×, NA = 0.8) and a Ti:sapphire laser (Spectra-Physics Mai Tai, excitation wavelength 920 nm). Images were taken at a zoom of 4.0 (pixel size 0.143 × 0.143 µm) and *Z*-step size of 0.7 µm. The mice received an i.p. injection of DOI (10 mg kg^{-1}) or TBG (50 mg kg^{-1}) immediately after they recovered from the anaesthesia of the first imaging session. The mice were re-imaged 24 h after drug administration. Dendritic spine dynamics were analysed using ImageJ. Spine formation and elimination were quantified as percentages of spine numbers on day 0.

Antidepressant-like response following unpredictable mild stress

Male and female mice (8 weeks old) were subjected to 7 d of unpredictable mild stress (UMS), as described previously[43]. In brief, the following stressors were used: day 1: light phase = 30 min of restraint stress × 2; dark phase = homecage space reduction. Day 2: light phase = exposure to a new room + 30 min on the orbital shaker, sudden loud noise × 5, tail suspension for 6 min; dark phase = wet bedding. Day 3: light phase = exposure to new mice; dark phase = exposure to light. Day 4: light phase = social isolation; dark phase = tilted cage. Day 5: light phase = tilted cage, island isolation; dark phase = no bedding. Day 6: light phase = no bedding, random puff of air × 5–10; dark phase = foreign objects. Day 7: light phase = foreign objects, food deprivation; dark phase = food deprivation, continual exposure to loud music. Immediately following UMS, TBG or vehicle were administered via i.p. injection, and 24 h later the mice were subjected to a FST using the same procedure as described below.

Forced swim test in the absence of UMS

Male C57/BL6J mice (9–10 weeks old at the time of the experiment) were obtained from the Jackson Laboratory and housed 4–5 mice per cage in a vivarium at UCD following an IACUC-approved protocol. After 1 week in the vivarium, each mouse was handled for approximately 1 min by a male experimenter for 3 consecutive days leading up to the first FST. All experiments were carried out by the same male experimenter who performed handling. During the FST, mice underwent a 6-min swim session in a clear Plexiglas cylinder 40 cm tall, 20 cm in diameter, and filled with 30 cm of 24 ± 1 °C water. Fresh water was used for each mouse. After handling and habituation to the experimenter, drug-naive mice first underwent a pre-test swim to more reliably induce a depressive phenotype in the subsequent FST sessions. Immobility scores for all mice were determined after the pre-test and mice were randomly assigned to treatment groups to generate groups with similar average immobility scores to be used for the following two FST sessions. The next day, the mice received i.p. injections of TBG (50 mg kg^{-1}), a positive control (ketamine, 3 mg kg^{-1}), or vehicle (saline). One additional group received ketanserin (4 mg kg^{-1} i.p.) 10 min before i.p. administration of TBG (50 mg kg^{-1}). The following day, the mice were subjected to the FST and then returned to their homecages. One week later, the FST was performed again to assess the sustained effects of the drugs. All FSTs were performed between the hours of 8:00 and 13:00. Experiments were video-recorded and manually scored offline. Immobility time—defined as passive floating or remaining motionless with no activity other than that needed to keep the head above water—was scored for the last 4 min of the 6 min trial.

Alcohol consumption

Male C57/BL6J mice (6–8 weeks old) were obtained from The Jackson Laboratory and were individually housed in a reverse light/dark cycle room (lights on 22:00–10:00). Temperature was kept constant at 22 ± 2 °C, and relative humidity was maintained at 50 ± 5%. Mice were given access to food and tap water ad libitum. After one week of habituation to the vivarium, the two-bottle-choice alcohol-drinking experiment was conducted as described previously[29]. For 7 weeks, mice were given intermittent access to alcohol in their homecage. On Mondays, Wednesdays and Fridays, two bottles were made available for 24 h: one containing 20% ethanol and another containing only water. On Tuesdays, Thursdays, Saturdays and Sundays, the mice were given access only to water. After 7 weeks, mice were administered TBG (50 mg kg^{-1}) or vehicle (saline) via i.p. injection 3 h before the beginning of a drinking session. Ethanol (g kg^{-1}) and water (ml kg^{-1}) intake were monitored during the first 4 h (initial binge), the first 24 h and the second 24 h. Next, the mice were given only water for 48 h before the start of another drinking session, during which ethanol and water consumption were monitored. The placement (right or left) of the bottles was altered in each session to control for side preference. Spillage was monitored using an additional bottle in a nearby unused cage. Alcohol preference was calculated as alcohol/(water + alcohol). Mice were tested using a counterbalanced, within-subject design with one

week of drug-free alcohol drinking regimen between treatments. One mouse was excluded because a bottle from which it was drinking was found to be leaking.

Sucrose preference

Male C57/BL6J mice were individually housed and subjected to a two-bottle choice experiment. First, mice were administered TBG (50 mg kg^{-1}) or vehicle (saline) via i.p. injection 3 h before the beginning of a two-bottle choice session. During this 3-h period, mice were not given access to water in an attempt to increase their thirst. At the start of the experiment, mice were given one bottle of water and one bottle of water containing 5% sucrose. Sucrose solution and water intake were monitored during the first 4 h and the first 24 h. Sucrose preference was calculated as the amount of sucrose solution consumed minus the amount of water consumed, divided by the total amount of liquid consumed.

Heroin self-administration behaviour

Subjects were age-matched male (n = 16) and female (n = 16) Wistar rats (Charles River). Rats were single-housed in a temperature- and humidity-controlled room with a 12 h light/dark cycle (7:00 lights on) with free access to standard laboratory chow and water. Two rats (one male and one female) were excluded from the final dataset owing to defective catheters to give a final n = 30 rats. Rats were surgically implanted with an intravenous catheter as previously described[44]. Heroin self-administration training began at least one week after surgery on a fixed ratio 1 (FR1) schedule of reinforcement. Operant chambers were equipped with both an active (heroin-delivering) and an inactive lever, and each heroin infusion (0.04 mg, 50 µl, 2.85 s) was coupled with delivery of a light cue located above the active lever and a 3.5 kHz tone (5 s). Both levers retracted upon initiation of a heroin infusion and remained retracted during the tone + light heroin cue presentation. After six self-administration sessions (2.5 h) on FR1, rats progressed to a variable ratio 5 (VR5) for three sessions and continued to the final variable ratio 15 (VR15) for five sessions. Rats then began extinction training. Extinction training sessions (1 h) were conducted in the same operant chambers (context) in which rats previously self-administered heroin, but in the absence of heroin and its tone + light cue. Both levers remained extended throughout the session, and responding was recorded but produced no consequence. After completing a total of 7 extinction sessions, rats underwent a cued reinstatement test (1 h, withdrawal day 10–12). During the cue test, the heroin tone + light cues were available but heroin was not. The first active lever press resulted in presentation of the heroin cues, and then cues were available on a VR5 schedule (active lever only) for the remainder of the test. Lever retraction occurred during cue presentation (as during self-administration). Injections of TBG (40 mg kg^{-1} i.p.) or vehicle were administered on the third VR15 session, the first extinction session and the cued reinstatement test. For each of these time points, TBG or vehicle was injected 30 min before placement in the chamber. Treatment groups were balanced on the basis of response rates, heroin intake and sex. Behavioural sessions were conducted daily (on weekdays only). Catheters were flushed after each self-administration session with cefazolin and taurolidine citrate solution to prevent infection and/or catheter occlusion. Statistical tests were performed in Prism (GraphPad Prism, RRID:SCR_002798; V8.0) software.

Sucrose self-administration behaviour

Sucrose self-administration procedures were designed to mimic heroin self-administration conditions. Subjects were age-matched male (n = 24) and female (n = 24) Wistar rats (Charles River). Rats were single-housed and had free access to standard laboratory chow and water throughout the experiment. Eight rats (seven males and one female) were excluded from the final dataset due to failure to acquire sucrose self-administration to give a final n = 40 rats. The final groups consisted of vehicle, SA (2.5), SA (10), SA (40), EXT (40) and CUE (40). The number of rats in each group was 7, 6, 7, 7, 7 and 6, respectively (40 rats total). At least one week after arrival and acclimatization to the animal facility, sucrose self-administration training began on a fixed ratio 1 (FR1) schedule of reinforcement. Operant chambers were equipped with an active (sucrose-delivering) and inactive lever, and each sucrose reward (45 mg pellet; Bio-Serv F0023) was coupled with the same tone + light cues used for the heroin study. Levers retracted upon pellet delivery and remained retracted during cue presentation (5 s). After six self-administration sessions (2 h) on FR1, rats progressed to a variable ratio 5 (VR5) for three sessions and continued to the final variable ratio 15 (VR15) for five sessions. Rats then began extinction training. Extinction training sessions (1 h) were conducted in the same operant chambers (context) in which animals previously self-administered sucrose, but neither sucrose nor the sucrose cues were available. Responding on both levers was recorded during each session, but produced no consequence. After completing 7 extinction sessions, rats underwent a cued reinstatement test (1 h). During the cue test, the sucrose tone + light cues were available but sucrose was not. The first active lever press resulted in presentation of the sucrose cues, and then cues were available on a VR5 schedule (active lever only) for the remainder of the test. Lever retraction occurred during cue presentation (as during self-administration). Injections were administered on the third VR15 session, the first extinction session, and the cued reinstatement test. For each of these tests, TBG (2.5 mg kg^{-1}, 10 mg kg^{-1}, or 40 mg kg^{-1} i.p.) or vehicle was injected 30 min before placement in the chamber. The low (2.5 mg kg^{-1}) and intermediate (10 mg kg^{-1}) doses of TBG were tested only on the third VR15 sucrose self-administration session. The high dose (40 mg kg^{-1}) was tested at all three test time points. Statistical tests were performed in Prism (GraphPad Prism, RRID:SCR_002798; V8.0) software.

Open-field test

Naive male (n = 7) and female (n = 6) Wistar rats (Charles River) were allowed to acclimatize to the animal facility for at least one week after arrival. Spontaneous locomotion in response to a novel open field (44 cm long × 36 cm wide × 43 cm tall) was assessed 30 min after injection of vehicle or TBG (40 mg kg^{-1}, i.p.). Videos were recorded with an overhead camera connected to the tracking software EthoVision XT (Noldus) for subsequent offline analysis. Rats were allowed to move freely in the open field for 30 min, then they were briefly removed from the apparatus to receive an injection of cocaine (15 mg kg^{-1}, i.p.). The rats were immediately returned to the open field for an additional hour to assess cocaine-induced locomotion. Each open-field chamber was cleaned with Clidox-S in between sessions. Locomotion was tracked using EthoVision XT to assess the velocity (cm s^{-1}) and total distance travelled (m) during the baseline (first 30 min) and cocaine (last 60 min) phases separately. Thigmotaxis—assessed as the percentage of time spent in the centre of the apparatus (26 cm long × 18 cm wide; that is, 9-cm perimeters)—was also analysed during the baseline period to determine whether TBG alters anxiety in the open field.

Reporting summary

Further information on research design is available in the Nature Research Reporting Summary linked to this paper.

Data availability

Data are available at https://doi.org/10.6084/m9.figshare.11634795. Source data are provided with this paper.

Code availability

Custom-written data analysis codes are available upon request from the corresponding author.

35. Langheinrich, U., Vacun, G. & Wagner, T. Zebrafish embryos express an orthologue of HERG and are sensitive toward a range of QT-prolonging drugs inducing severe arrhythmia. *Toxicol. Appl. Pharmacol.* **193**, 370–382 (2003).
36. Sampurna, B. P., Audira, G., Juniardi, S., Lai, Y.-H. & Hsiao, C.-D. A simple ImageJ-based method to measure cardiac rhythm in zebrafish embryos. *Inventions* **3**, 21 (2018).
37. Westerfield, M. *The zebrafish book. A guide for the laboratory use of zebrafish (*Danio rerio*)* 5th edn (Univ. Oregon Press, 2007).
38. Ahrens, M. B., Orger, M. B., Robson, D. N., Li, J. M. & Keller, P. J. Whole-brain functional imaging at cellular resolution using light-sheet microscopy. *Nat. Methods* **10**, 413–420 (2013).
39. Kroeze, W. K. et al. PRESTO-Tango as an open-source resource for interrogation of the druggable human GPCRome. *Nat. Struct. Mol. Biol.* **22**, 362–369 (2015).
40. Barupal, D. K. et al. A comprehensive plasma metabolomics dataset for a cohort of mouse knockouts within the international mouse phenotyping consortium. *Metabolites* **9**, 101 (2019).
41. Feng, G. et al. Imaging neuronal subsets in transgenic mice expressing multiple spectral variants of GFP. *Neuron* **28**, 41–51 (2000).
42. Xu, T. et al. Rapid formation and selective stabilization of synapses for enduring motor memories. *Nature* **462**, 915–919 (2009).
43. Chen, C. C., Lu, J., Yang, R., Ding, J. B. & Zuo, Y. Selective activation of parvalbumin interneurons prevents stress-induced synapse loss and perceptual defects. *Mol. Psychiatry* **23**, 1614–1625 (2018).
44. Vazquez, M., Frazier, J. H., Reichel, C. M. & Peters, J. Acute ovarian hormone treatment in freely cycling female rats regulates distinct aspects of heroin seeking. *Learn. Mem.* **27**, 6–11 (2020).

Acknowledgements This work was supported by funds from the National Institutes of Health (NIH) (R01GM128997 to D.E.O.; R37AA01684 to D.R.; R01AA022583 to D.K.; R01MH109475, R01MH104227 and R01NS104950 to Y.Z.; R01DA045836 to J.P.; and U19AG023122 to O.F.), a Hellman Fellowship (D.E.O.), UC Davis STAIR and STAIR Plus grants (D.E.O.), a Max Planck Fellowship at MPFI (Y.Z.), four NIH training grants (T32GM113770 to R.J.T., T32MH112507 to L.P.C., 5T32GM099608 to M.V.V., and 4T32GM6754714 to D.M.-T.), two UC Davis Provost's Undergraduate Fellowships (to J.V. and A.J.P.), the Paul G. Allen Family Foundation (M.N.M. and D.K.), the Genentech Fellowship Program (D.M.-T.), and a Medical College of Wisconsin Research Affairs Counsel Pilot Grant (J.D.M.). B.M.B. was supported by the National Center for Advancing Translational Sciences, National Institutes of Health, through grant number UL1 TR001860 and linked award TL1 TR001861. Delix Therapeutics funded the large receptor screen conducted at Eurofins Discovery. We thank F. F. Wagner for help in coordinating with Eurofins Discovery. This project used the Biological Analysis Core of the UC Davis MIND Institute Intellectual and Development Disabilities Research Center (U54 HD079125). The Olympus FV1000 confocal microscope used in this study was purchased using NIH Shared Instrumentation Grant 1S10RR019266-01. We thank the MCB Light Microscopy Imaging Facility, which is a UC Davis Campus Core Research Facility, for the use of this microscope. Several of the drugs used in this study were provided by the NIDA Drug Supply Program. We thank D. R. Carty for assistance with larval zebrafish toxicity assays.

Author contributions A.J.P., Z.Q.H. and G.Z. synthesized the ibogalogs. L.E.D. synthesized 5-MeO-DMT fumarate and performed the CNS MPO calculations. L.P.C. performed the dendritogenesis and spinogenesis assays. L.P.C. and J.V. performed the head-twitch response experiments. M.N.M. performed the zebrafish heart-rate and seizure experiments. J.C.T., D.M.-T. and R.J.T. performed the zebrafish behavioural experiments. R.J.T. and B.Y. performed the zebrafish toxicity assays. B.M.B. and L.P.C. performed the hERG inhibition studies. L.P.C. performed the solubility studies and conditioned place preference experiments. J.L., T.L. and L.P.C. performed the experiments assessing in vivo spine dynamics. L.J.L., E.I.A. and J.D.M. performed the receptor functional assays. J.L. and M.T. performed the forced swim test following UMS. M.V.V. performed the forced swim test study without UMS with assistance from L.E.D. Z.T.R. and L.P.C. performed the pharmacokinetic studies. J.P. performed the heroin self-administration experiments. Y.E. performed the alcohol consumption assays. L.P.C. performed the sucrose preference assay. O.F., H.W., J.D.M., P.J.L., D.K., D.R., J.P., Y.Z. and D.E.O. supervised various aspects of this project and assisted with data analysis. D.E.O. conceived the project and wrote the manuscript with input from all authors.

Competing interests D.E.O. is the president and chief scientific officer of Delix Therapeutics. Delix Therapeutics has licensed TBG-related technology from the University of California, Davis.

Additional information

Supplementary information is available for this paper at https://doi.org/10.1038/s41586-020-3008-z.

Correspondence and requests for materials should be addressed to D.E.O.

Peer review information *Nature* thanks Amy Newman, Yavin Shaham and the other, anonymous, reviewer(s) for their contribution to the peer review of this work.

Reprints and permissions information is available at http://www.nature.com/reprints.

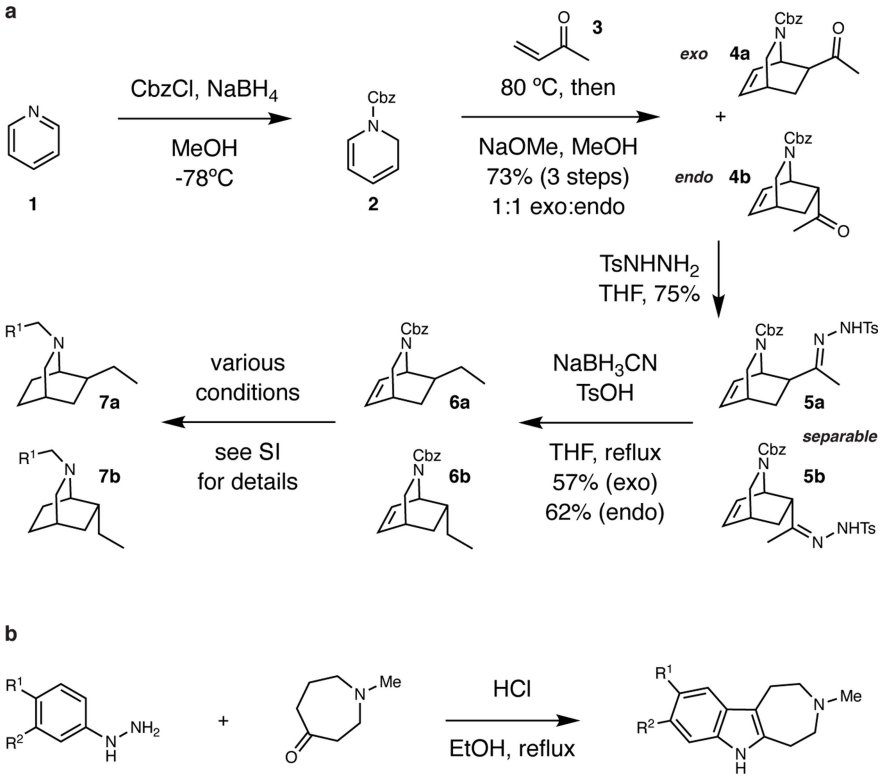

Extended Data Fig. 1 | Synthesis of ibogalogs. a, Ibogalogs lacking the tetrahydroazepine of ibogaine were synthesized in only a few steps. In brief, acylation of pyridine **1** under reductive conditions yielded the carboxybenzyl (Cbz)-protected dihydropyridine **2**, which was immediately subjected to a Diels–Alder reaction with methyl vinyl ketone (**3**) followed by an in situ epimerization with NaOMe to afford an inseparable 1:1 mixture of *exo* (**4a**) and *endo* (**4b**) isomers (73% over 3 steps). Reaction of **4a** and **4b** with tosylhydrazide yielded the hydrazones **5a** and **5b**, which were separable via a combination of selective crystallization and chromatography (total yield of the two isomers, 75%). Caglioti reduction of the tosylhydrazones yielded **6a** or **6b**, which were readily converted to a variety of analogues via reaction sequences involving hydrogenolysis of the Cbz group, hydrogenation of the olefin, and C–N bond formation (Supplementary Information). **b**, Ibogalogs lacking the isoquinuclidine of ibogaine were synthesized in a single step through Fischer indole cyclization. See Supplementary Information for details.

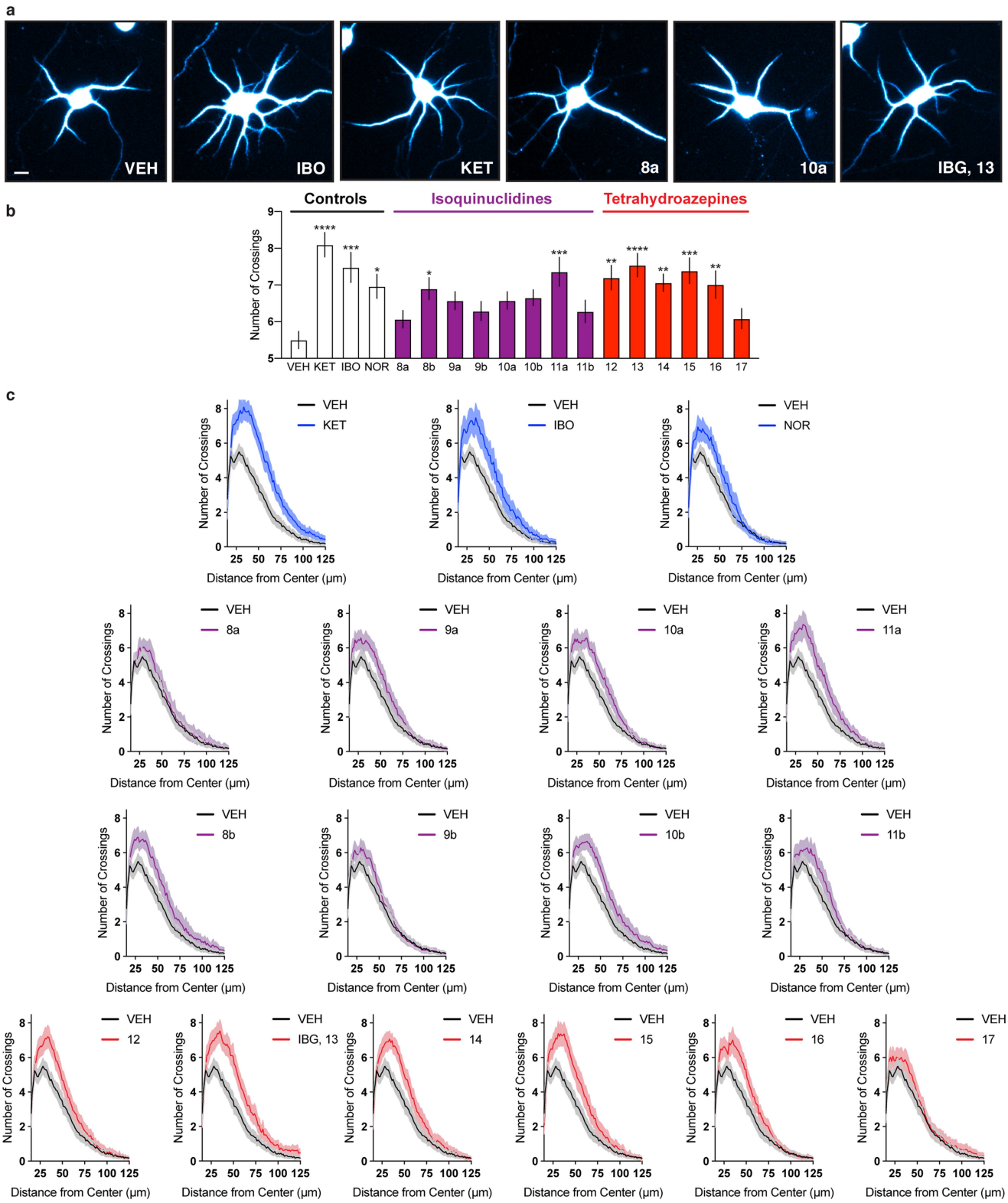

Extended Data Fig. 2 | The effects of ibogalogs on dendritogenesis. **a**, Representative images of rat embryonic cortical neurons (DIV6) treated with the indicated compounds. Scale bar, 10 μm. **b**, Maximum numbers of crossings (N_{max}) of the Sholl plots demonstrate that tetrahydroazepine-containing ibogalogs are more effective at increasing dendritic arbor complexity than are isoquinuclicine-containing ibogalogs. **c**, Sholl analysis (circle radii, 1.34-μm increments) demonstrates that cultured cortical neurons treated with several ibogalogs have more complex dendritic arbors compared to vehicle control (n = 52–83 neurons per treatment). The shaded area surrounding each line represents 95% confidence intervals. Control compounds, isoquinuclidines and tetrahydroazepines are shown in blue, purple and red, respectively. Exact n values for each experimental condition are reported in Supplementary Table 1. Specific statistical tests, information on reproducibility, and exact P values are reported in Methods and Supplementary Table 1.

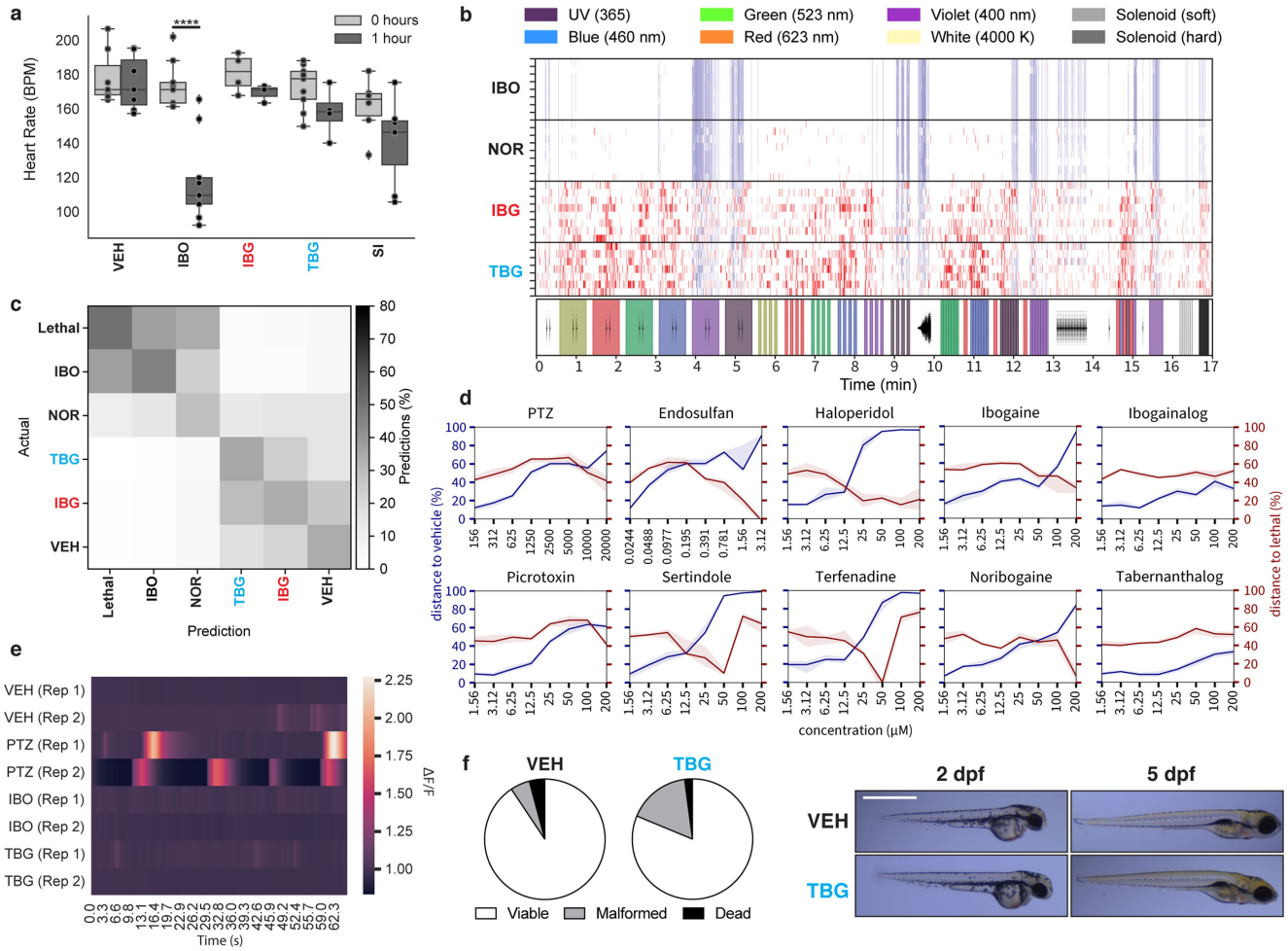

Extended Data Fig. 3 | TBG is safer than ibogaine. a, Unlike ibogaine, IBG and TBG do not induce bradycardia in larval zebrafish. Sertindole (SI) was used as a positive control. **b**, Heat maps are shown representing aggregate larval zebrafish locomotor activity per well compared to vehicle controls (pseudo-*Z*-score). Red and blue indicate higher and lower activity than the mean of vehicle controls, respectively, while white indicates activity within ±1 s.d. of the control. Stimuli applied over time are indicated under the heat maps. Colours indicate bright LED light of respective colours, black traces represent the waveforms of acoustic stimuli, and grey vertical lines indicate physical tapping as secondary acoustic stimuli. **c**, Confusion matrix for classification of compounds (200 μM) plus vehicle and lethal controls. **d**, Concentration–response curves are shown for treated zebrafish subjected to the series of stimuli depicted in **b**. Lower percentages indicate treatments that were more often classified as vehicle (blue) or lethal (red). The solid line denotes the median and the shading denotes a 95th percentile confidence interval calculated by bootstrap. $n = 8$ wells per condition (64 zebrafish per condition). Blue lines indicate that all compounds produce behavioural phenotypes more distinct from vehicle at higher concentrations. Red lines indicate that known toxins (for example, PTZ, picrotoxin, endosulfan), known hERG inhibitors (sertindole, haloperidol, terfenadine) and iboga alkaloids (IBO, NOR) produce behavioural phenotypes more closely resembling a lethal phenotype as their concentrations are increased. Increasing concentrations of IBG or TBG do not produce lethal-like behavioural phenotypes. **e**, Transgenic larval zebrafish expressing GCaMP5G were immobilized in agarose, treated with compounds, and imaged over time. The known seizure-inducing compound PTZ was used as a positive control. Ibogaine and TBG were treated at 50 μM ($n = 2$ per condition). **f**, Proportion of viable and non-viable (malformed + dead) zebrafish following treatment with vehicle and TBG (66 μM) for 5 dpf (Fisher's exact test: $P = 0.3864$). Representative images of zebrafish treated with vehicle and TBG (66 μM) for 2 and 5 dpf are shown. Scale bar, 2 mm. Exact *n* values for each experimental condition are reported in Supplementary Table 1. Specific statistical tests, information on reproducibility and exact *P* values are reported in the Methods and Supplementary Table 1.

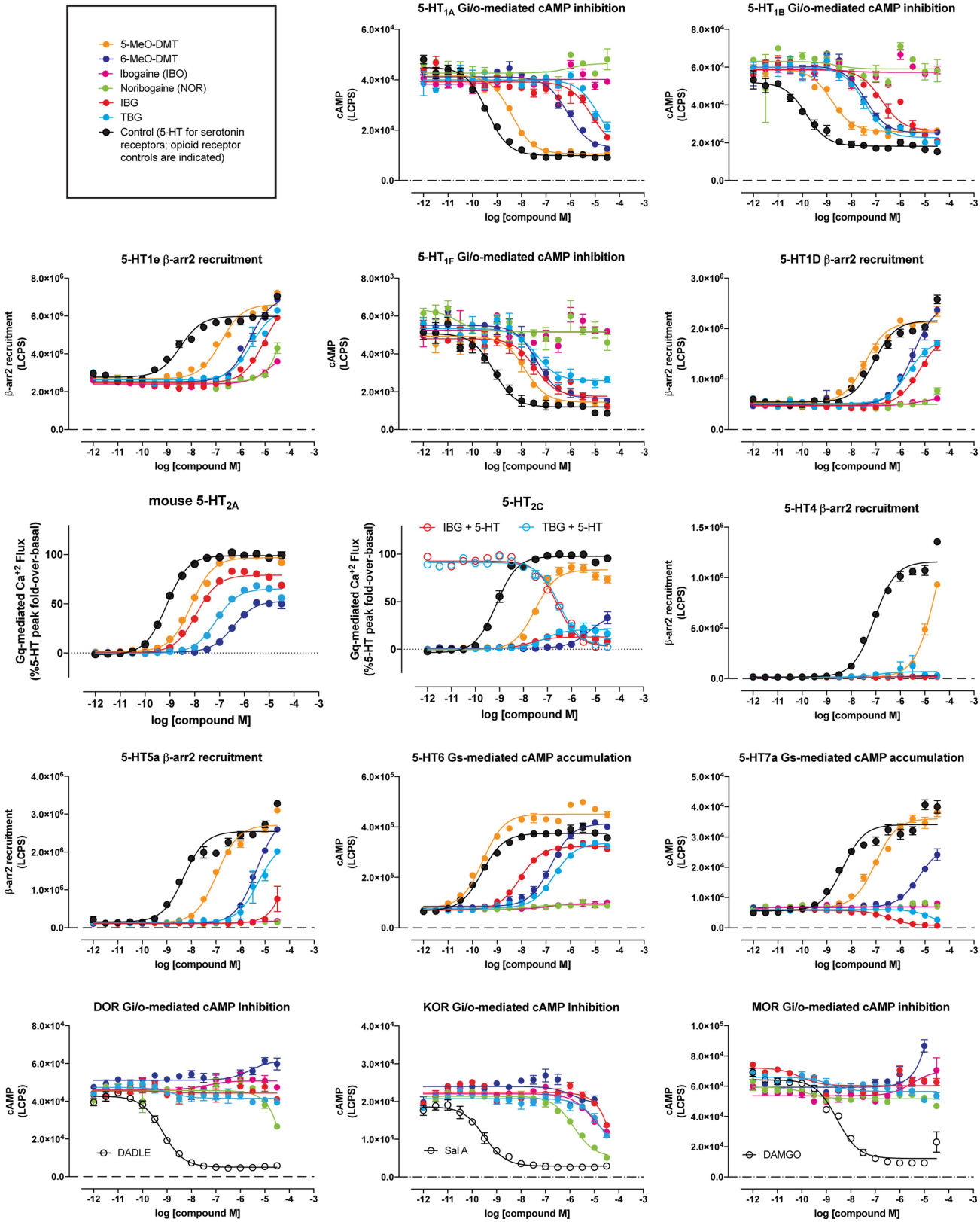

Extended Data Fig. 4 | Concentration–response curves demonstrating the abilities of ibogalogs and related compounds to activate 5-HT and opioid receptors. All compounds were assayed in parallel using the same drug dilutions. Graphs reflect representative concentration–response curves plotting mean and s.e.m. of data points performed in duplicate or triplicate. Assay details are described in Methods. Exact *n* values for each experimental condition are reported in Supplementary Table 1. Specific statistical tests, information on reproducibility and exact *P* values are reported in Methods and in Supplementary Table 1.

	5-MeO-DMT			6-MeO-DMT			IBG			TBG			IBO			NOR		
Target Receptor	EC_{50}, nM	E_{max} % Control	$\log(E_{max}/EC_{50})$	EC_{50}, nM	E_{max} % Control	$\log(E_{max}/EC_{50})$	EC_{50}, nM	E_{max} % Control	$\log(E_{max}/EC_{50})$	EC_{50}, nM	E_{max} % Control	$\log(E_{max}/EC_{50})$	EC_{50}, nM	E_{max} % Control	$\log(E_{max}/EC_{50})$	EC_{50}, nM	E_{max} % Control	$\log(E_{max}/EC_{50})$
5-HT1A	3.92	98	8.40	725.40	91	6.10	6911.00	91	5.12	14600.0	95	4.81	Inactive	Inactive	Inactive	Inactive	Inactive	Inactive
5-HT1B	1.53	78	8.71	37.06	85	7.36	170.40	76	6.65	33.66	87	7.41	Inactive	Inactive	Inactive	Inactive	Inactive	Inactive
5-HT1D	37.01	98	7.42	3246.00	120	5.57	6043.00	82	5.13	2180.00	76	5.54	Inactive	Inactive	Inactive	Inactive	Inactive	Inactive
5-HT1e	160.20	119	6.87	2363.00	131	5.74	9309.00	126	5.13	2784.00	117	5.62	Inactive	Inactive	Inactive	Inactive	Inactive	Inactive
5-HT1F	14.00	93	7.82	44.50	88	7.30	35.10	85	7.38	40.40	64	7.20	Inactive	Inactive	Inactive	Inactive	Inactive	Inactive
5-HT2A	1.85	82	8.65	1003.00	63	5.80	18.10	82	7.66	147.00	57	6.59	Inactive	Inactive	Inactive	Inactive	Inactive	Inactive
5-HT2B	5.87	73	8.09	Inactive	Inactive	Inactive	Inactive	Inactive	Inactive	Inactive	Inactive	Inactive	Inactive	Inactive	Inactive	Inactive	Inactive	Inactive
5-HT2C	30.70	84	7.44	5358.00	36	4.83	19.00	13	6.84	68.50	21	6.49	Inactive	Inactive	Inactive	Inactive	Inactive	Inactive
5-HT4	>10,000	N.D.	<5.00	>10,000	N.D.	<5.00	>10,000	N.D.	<5.00	>10,000	N.D.	<5.00	Inactive	Inactive	Inactive	Inactive	Inactive	Inactive
5-HT5a	110.00	107	6.99	4543.00	117	5.41	>10,000	N.D.	<5.00	>10,000	N.D.	<5.00	Inactive	Inactive	Inactive	Inactive	Inactive	Inactive
5-HT6	0.24	125	9.72	162.00	113	6.84	8.80	83	7.97	214.00	87.5	6.61	Inactive	Inactive	Inactive	Inactive	Inactive	Inactive
5-HT7a	65.70	107	7.21	5653.00	75	5.12	335.00	-17	N.D.	>10,000	N.D.	N.D.	N.D.	N.D.	N.D.	N.D.	N.D.	N.D.
MOR	Inactive	Inactive	Inactive	Inactive	Inactive	Inactive	Inactive	Inactive	Inactive	Inactive	Inactive	Inactive	Inactive	Inactive	Inactive	Inactive	Inactive	Inactive
KOR	Inactive	Inactive	Inactive	>10,000	N.D.	<5.00	>10,000	N.D.	<5.00	>10,000	N.D.	<5.00	>10,000	N.D.	<5.00	1400	85	5.78
DOR	Inactive	Inactive	Inactive	Inactive	Inactive	Inactive	Inactive	Inactive	Inactive	Inactive	Inactive	Inactive	Inactive	Inactive	Inactive	Inactive	Inactive	Inactive

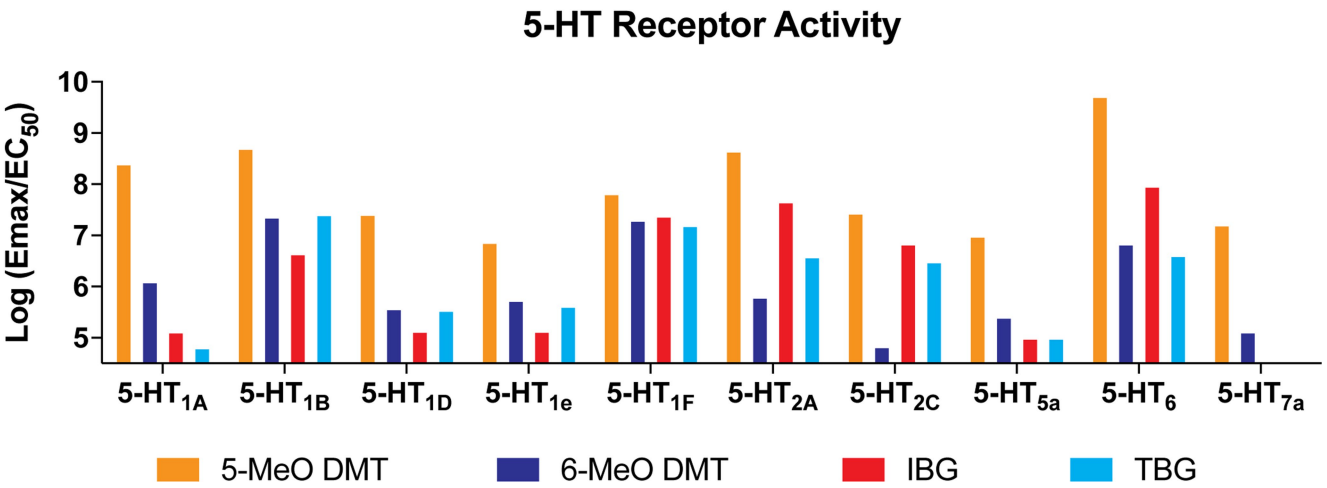

Extended Data Fig. 5 | Pharmacological profiles of ibogalogs and related compounds. EC_{50} and E_{max} estimates from at least two independent concentration-response curves performed in duplicate or triplicate. $\log(E_{max}/EC_{50})$ activity relative to the system E_{max}. Inactive, inactive in agonist mode; N.D., not determined; blue boxes indicate that the compound exhibits antagonist activity; dark grey boxes indicate that the compound is inactive in agonist mode but not tested in antagonist mode; orange boxes indicate that the compound is an inverse agonist. Ibogalogs are more selective 5-HT_{2A} agonists than is 5-MeO-DMT. Exact *n* values for each experimental condition are reported in Supplementary Table 1. Specific statistical tests, information on reproducibility and exact *P* values are reported in Methods and in Supplementary Table 1.

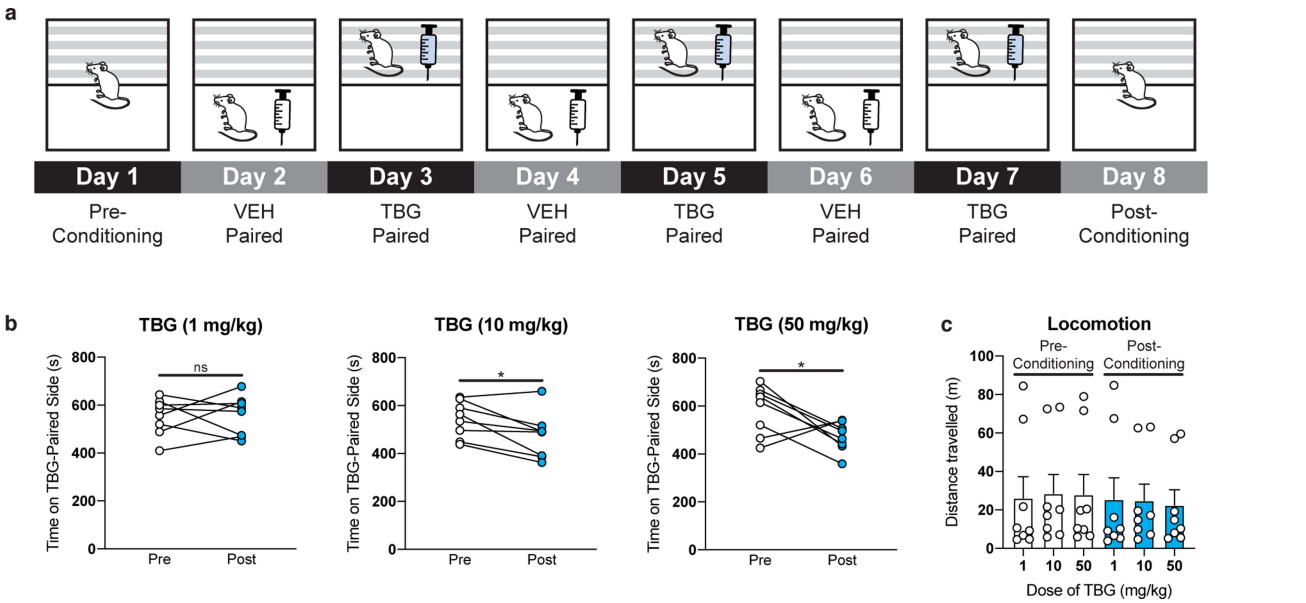

Extended Data Fig. 6 | High doses of TBG do not produce a conditioned place preference. a, Schematic of the design of the conditioned place preference experiments. On day 1, the amount of time the mice spent in each distinct side of a two-chamber apparatus was recorded. Next, vehicle and TBG were administered to mice on alternating days while they were confined to chamber A (white box) or chamber B (grey parallel lines), respectively. Conditioning lasted for a total of 6 days. On day 8, preference for each distinct side of the two-chamber apparatus was assessed. **b**, A low dose of TBG (1 mg kg^{-1}) did not produce conditioned place preference or conditioned place aversion. Higher doses (10 and 50 mg kg^{-1}) produce a modest conditioned place aversion. **c**, TBG does not produce any long-lasting (>24 h) effects on locomotion. There is no statistical difference in locomotion between any pre- or post-conditioning groups ($P = 0.9985$, one-way ANOVA). White bars indicate groups before receiving TBG (that is, pre-conditioning), and blue bars indicate groups 24 h after the last TBG administration (that is, post-conditioning). Exact *n* values for each experimental condition are reported in Supplementary Table 1. Specific statistical tests, information on reproducibility and exact *P* values are reported in Methods and in Supplementary Table 1.

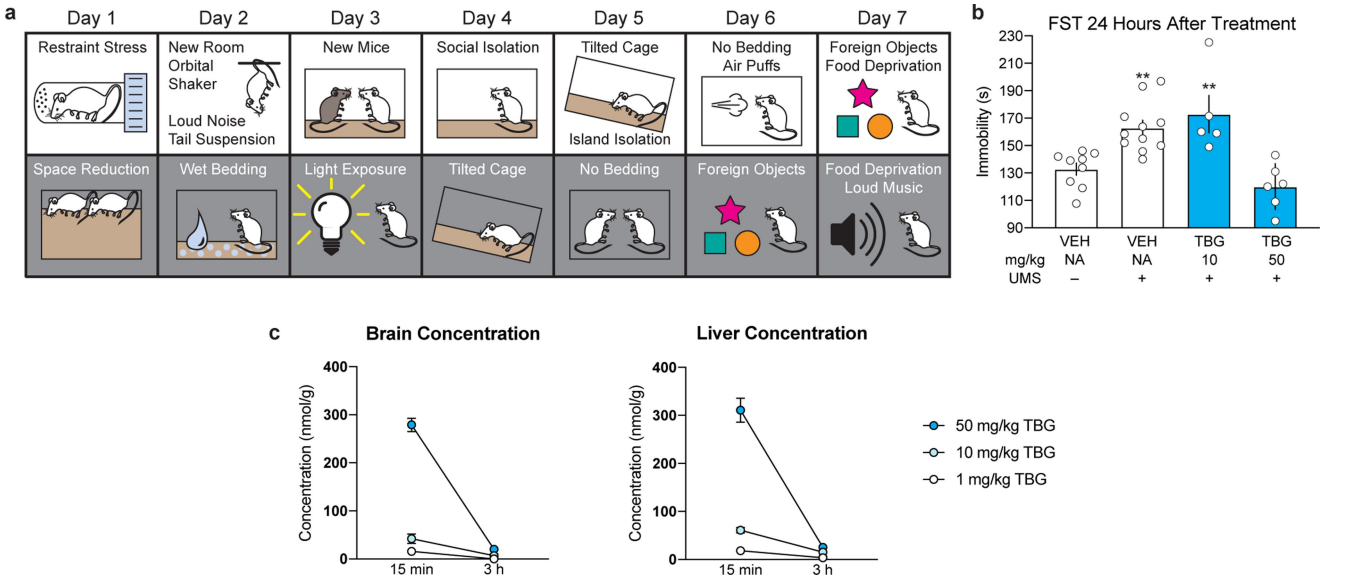

Extended Data Fig. 7 | TBG produces antidepressant effects in mice. **a**, Schematic illustrating the stressors used as part of the 7-day UMS protocol. White and grey boxes represent the light and dark phases of the light cycle, respectively. **b**, TBG rescues the effects of UMS on immobility. **c**, TBG (50 mg kg^{-1}) reaches high brain concentrations and is rapidly eliminated from the body. Mice were administered 3 different doses of TBG via i.p. injection and euthanized either 15 min or 3 h later. Whole brains and livers were collected, dried, homogenized and extracted with MTBE. Quantification was accomplished using LC–MS and concentrations of TBG in the two organs were calculated. Several samples for the 10 and 1 mg kg^{-1} doses at the 3 h time point had TBG at levels below the limit of quantification (around 5 nmol g^{-1}). In those cases, the values were recorded as 0. Exact *n* numbers for each experimental condition are reported in Supplementary Table 1. Specific statistical tests, information on reproducibility and exact *P* values are reported in Methods and in Supplementary Table 1.

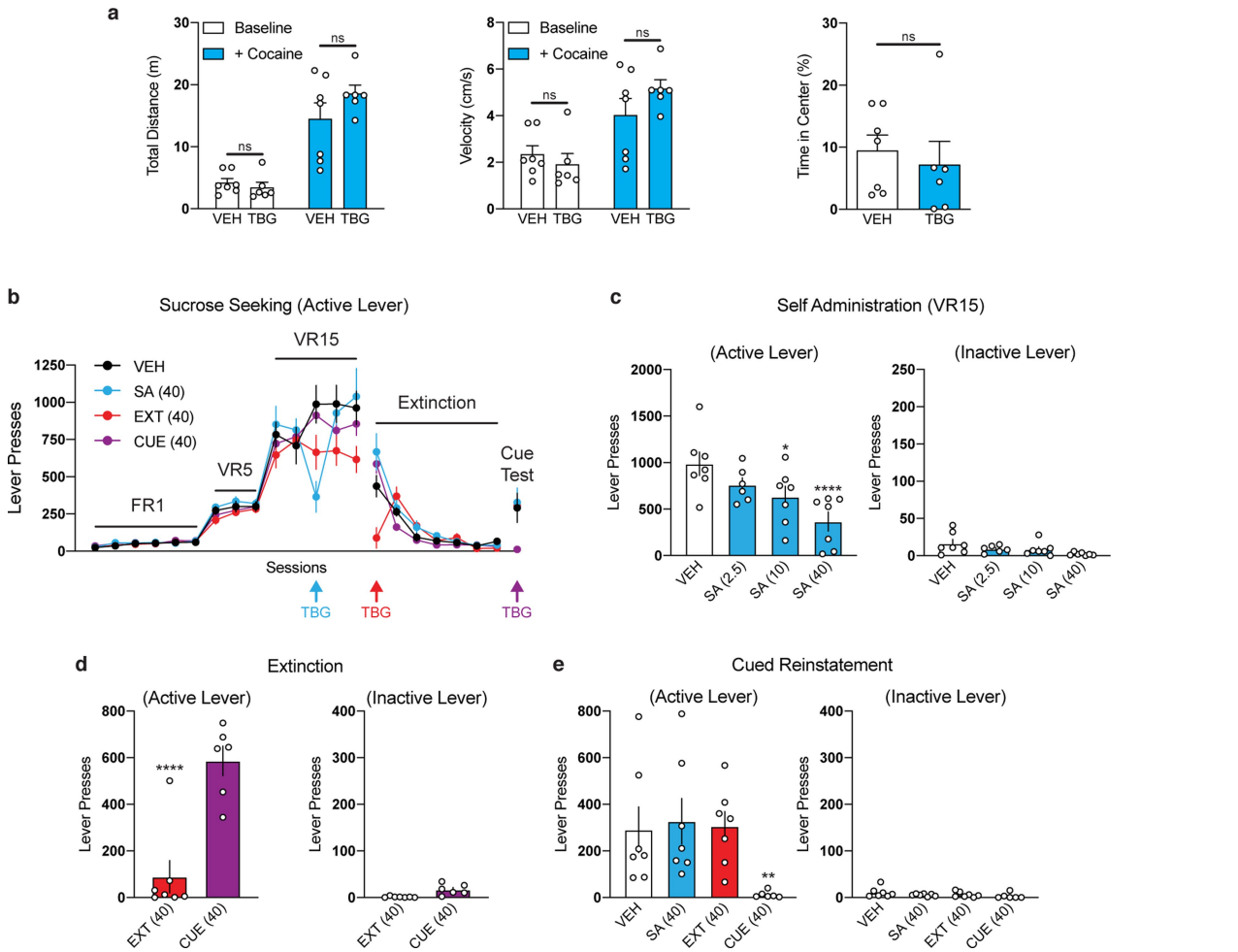

Extended Data Fig. 8 | Effects of TBG on locomotion and sucrose-seeking behaviour in rats. a, Acute administration of TBG does not impair locomotion in the open field. Rats were subjected to novelty-induced locomotion (baseline) for 30 min. At that time, cocaine was administered and psychostimulant-induced locomotion (+cocaine) was assessed for 60 min. There were no differences between the vehicle- and TBG-treated groups with respect to total distance travelled or average velocity. Furthermore, there was no difference in thigmotaxis measured during the baseline period (that is, the percentage of time in the centre of the open field). **b**–**e**, A sucrose self-administration experiment was conducted in a similar manner to the heroin self-administration experiment in Fig. 4. Doses in mg kg^{-1} are shown in parentheses. **b**, Sucrose seeking over time is shown. Coloured arrows indicate when each group received TBG. VEH was administered at all other time points to each group. **c**, TBG acutely reduces sucrose-seeking behaviour in a dose-dependent manner when administered during self-administration. **d**, TBG acutely reduces sucrose seeking when administered immediately before the first extinction session. The CUE (injection 1 = vehicle; injection 2, vehicle) and EXT (injection 1, vehicle; injection 2, TBG) groups were compared, as they were matched for the number of withdrawal days between the last self-administration and first extinction session. **e**, TBG does not have long-lasting effects on sucrose-seeking behaviour, as it does not reduce active lever pressing during the cued reinstatement when administered 12–14 days previously during self-administration (SA) or immediately before extinction (EXT). Exact *n* values for each experimental condition are reported in Supplementary Table 1. Specific statistical tests, information on reproducibility and exact *P* values are reported in Methods and in Supplementary Table 1.

Extended Data Table 1 | TBG and IBG are more soluble than ibogaine

a

Solubility at [Cmpd] (mg/mL)			
Cmpd	40	8	4
IBO	no ✗	no ✗	no ✗
IBG	yes ✓	yes ✓	yes ✓
TBG	yes ✓	yes ✓	yes ✓

b

Vehicle Conditions	Concentration	Soluble?
Saline + 10% EtOH + 10% DMSO	40 mg/ml	NO ✗
Saline + 10% EtOH	8 mg/ml	NO ✗
Saline + 10% DMSO	8 mg/ml	NO ✗
Saline + 10% EtOH + 10% DMSO	8 mg/ml	NO ✗
Saline + 10% EtOH + 10% Kolliphor	8 mg/ml	NO ✗
Saline + 10% EtOH + 20% Kolliphor	8 mg/ml	NO ✗
Saline + 10% EtOH + 25% Kolliphor	8 mg/ml	NO ✗
Saline + 10% EtOH + 30% Kolliphor	8 mg/ml	NO ✗
Saline + 10% EtOH + 40% Kolliphor	8 mg/ml	NO ✗
Saline + 10% DMSO + 10% Kolliphor	8 mg/ml	NO ✗
Saline + 10% DMSO + 25% Kolliphor	8 mg/ml	NO ✗
Saline + 10% DMSO + 15% Glycerol	8 mg/ml	NO ✗
Saline + 10 mM ATP	8 mg/ml	NO ✗
Saline + 10% DMSO	4 mg/ml	NO ✗
Saline + 10% DMSO + 25% Kolliphor	4 mg/ml	NO ✗
Saline + 10% DMSO	1 mg/ml	YES ●

a, The fumarate salts of TBG and IBG are readily soluble in saline (0.9%), whereas ibogaine hydrochloride is not.
b, Ibogaine hydrochloride exhibits limited solubility in various saline-based vehicles. Solutions of saline (0.9%) containing various percentages of co-solvents/additives were added to finely crushed ibogaine hydrochloride. All of our attempts to improve its solubility through pulverizing, sonication, and mild heating (<50 °C) were unsuccessful. Moreover, the addition of co-solvents (ethanol, dimethyl sulfoxide, glycerol), surfactants (Kolliphor), or hydrotropes (ATP) to the vehicle did not substantially improve its solubility. We confirmed the purity and identity of the ibogaine hydrochloride used in these studies through a combination of NMR, LC–MS, and X-ray crystallography experiments. Exact *n* values for each experimental condition are reported in Supplementary Table 1. Specific statistical tests, information on reproducibility and exact *P* values are reported in Methods and in Supplementary Table 1.

Extended Data Table 2 | Safety pharmacology screen

Eurofins Catalog #	Assay Name	Species	% Inhibition
107710	ATPase, Na+/K+, Heart, Pig	pig	-9
104010	Cholinesterase, Acetyl, ACES	human	13
116030	Cyclooxygenase COX-1	human	16
118030	Cyclooxygenase COX-2	human	7
140010	Monoamine Oxidase MAO-A	human	66
140120	Monoamine Oxidase MAO-B	human	16
107300	Peptidase, Angiotensin Converting Enzyme	rabbit	2
112510	Peptidase, CTSG (Cathepsin G)	human	-2
152300	Phosphodiesterase PDE3A	human	6
154420	Phosphodiesterase PDE4D2	human	1
200510	Adenosine A1	human	-4
200610	Adenosine A2A	human	-8
203110	Adrenergic α1A	human	15
203210	Adrenergic α1B	human	20
203400	Adrenergic α1D	human	15
203630	Adrenergic α2A	human	81
203710	Adrenergic α2B	human	27
204010	Adrenergic β1	human	9
204110	Adrenergic β2	human	9
206000	Androgen (Testosterone)	human	6
210030	Angiotensin AT1	human	3
212620	Bradykinin B2	human	9
214510	Calcium Channel L-Type, Benzothiazepine	rat	18
214600	Calcium Channel L-Type, Dihydropyridine	rat	6
215000	Calcium Channel L-Type, Phenylalkylamine	rat	42
216000	Calcium Channel N-Type	rat	-3
217050	Cannabinoid CB1	human	1
217100	Cannabinoid CB2	human	-21
217510	Chemokine CCR1	human	11
244500	Chemokine CXCR2 (IL-8RB)	human	-2
219500	Dopamine D1	human	3
219600	Dopamine D2L	human	18
219700	Dopamine D2S	human	0
224010	Endothelin ETA	human	8
226010	Estrogen ERα	human	1
226810	GABAA, Chloride Channel, TBOB	rat	-1
226600	GABAA, Flunitrazepam, Central	rat	-2
226630	GABAA, Ro-15-1788, Hippocampus	rat	10
228610	GABAB1A	human	0
232030	Glucocorticoid	human	12
232600	Glutamate, AMPA	rat	8
232710	Glutamate, Kainate	rat	8
237000	Glutamate, Metabotropic, mGlu5	human	1
232810	Glutamate, NMDA, Agonism	rat	0
232910	Glutamate, NMDA, Glycine	rat	2
233000	Glutamate, NMDA, Phencyclidine	rat	3
234000	Glutamate, NMDA, Polyamine	rat	-2
239000	Glycine, Strychnine-Sensitive	rat	19
239610	Histamine H1	human	35
239710	Histamine H2	human	-12
250460	Leukotriene, Cysteinyl CysLT1	human	3
251100	Melanocortin MC1	human	-3
251350	Melanocortin MC4	human	-8
252610	Muscarinic M1	human	2
252710	Muscarinic M2	human	13
252810	Muscarinic M3	human	18
252910	Muscarinic M4	human	7
257010	Neuropeptide Y Y1	human	16
258700	Nicotinic Acetylcholine α1, Bungarotoxin	human	19
258730	Nicotinic Acetylcholine α3β4	human	16
260130	Opiate δ1 (OP1, DOP)	human	14
260210	Opiate κ (OP2, KOP)	human	7
260410	Opiate μ (OP3, MOP)	human	17
299037	Platelet Activating Factor (PAF)	human	7
265600	Potassium Channel [KATP]	hamster	6
265900	Potassium Channel hERG	human	28
267500	PPARγ	human	-6
299005	Progesterone PR-B	human	4
271110	Serotonin (5-Hydroxytryptamine) 5-HT1A	human	39
271230	Serotonin (5-Hydroxytryptamine) 5-HT1B	human	66
271650	Serotonin (5-Hydroxytryptamine) 5-HT2A	human	57
271700	Serotonin (5-Hydroxytryptamine) 5-HT2B	human	86
271800	Serotonin (5-Hydroxytryptamine) 5-HT2C	human	99
271910	Serotonin (5-Hydroxytryptamine) 5-HT3	human	14
279510	Sodium Channel, Site 2	rat	24
255520	Tachykinin NK1	human	18
202000	Transporter, Adenosine	guinea pig	-9
226400	Transporter, GABA	rat	1
274030	Transporter, SERT	human	88
287530	Vasopressin V1A	human	-6
252030	Transporter, Vesicular Monoamine (Non-Selective)	human	10

The effects of TBG (10 μM) on a wide range of targets was assessed by Eurofins Discovery. Assays were conducted in duplicate and the results were averaged. Targets with ≥50% inhibition are highlighted in blue. Exact *n* values for each experimental condition are reported in Supplementary Table 1. Specific statistical tests, information on reproducibility and exact *P* values are reported in Methods and in Supplementary Table 1.

nature research

Corresponding author(s): David E. Olson

Last updated by author(s): 10/12/2020

Reporting Summary

Nature Research wishes to improve the reproducibility of the work that we publish. This form provides structure for consistency and transparency in reporting. For further information on Nature Research policies, see Authors & Referees and the Editorial Policy Checklist.

Statistics

For all statistical analyses, confirm that the following items are present in the figure legend, table legend, main text, or Methods section.

n/a	Confirmed	
☐	☒	The exact sample size (*n*) for each experimental group/condition, given as a discrete number and unit of measurement
☒	☐	A statement on whether measurements were taken from distinct samples or whether the same sample was measured repeatedly
☐	☒	The statistical test(s) used AND whether they are one- or two-sided *Only common tests should be described solely by name; describe more complex techniques in the Methods section.*
☒	☐	A description of all covariates tested
☐	☒	A description of any assumptions or corrections, such as tests of normality and adjustment for multiple comparisons
☐	☒	A full description of the statistical parameters including central tendency (e.g. means) or other basic estimates (e.g. regression coefficient) AND variation (e.g. standard deviation) or associated estimates of uncertainty (e.g. confidence intervals)
☐	☒	For null hypothesis testing, the test statistic (e.g. *F*, *t*, *r*) with confidence intervals, effect sizes, degrees of freedom and *P* value noted *Give P values as exact values whenever suitable.*
☒	☐	For Bayesian analysis, information on the choice of priors and Markov chain Monte Carlo settings
☒	☐	For hierarchical and complex designs, identification of the appropriate level for tests and full reporting of outcomes
☐	☒	Estimates of effect sizes (e.g. Cohen's *d*, Pearson's *r*), indicating how they were calculated

Our web collection on statistics for biologists contains articles on many of the points above.

Software and code

Policy information about availability of computer code

Data collection	We have included a code availability statement. Zeiss Axiozoom.V16 and Zen software V2 blue edition were used for collection of zebrafish seizure data.
Data analysis	GraphPad Prism (version 8.1.2), ImageJ 2.0, Marvin Sketch (19.25.0), ImageJ plugin Time Series Analyzer V3, SciPy package “find_peaks”, ANYmaze software (version 6.2), TraceFinder 4.1, GraphPad Prism, RRID:SCR_002798; V8.0), EthoVision XT 14

For manuscripts utilizing custom algorithms or software that are central to the research but not yet described in published literature, software must be made available to editors/reviewers. We strongly encourage code deposition in a community repository (e.g. GitHub). See the Nature Research guidelines for submitting code & software for further information.

Data

Policy information about availability of data

All manuscripts must include a data availability statement. This statement should provide the following information, where applicable:

- Accession codes, unique identifiers, or web links for publicly available datasets
- A list of figures that have associated raw data
- A description of any restrictions on data availability

Data are available at the following link https://doi.org/10.6084/m9.figshare.11634795.

Field-specific reporting

Please select the one below that is the best fit for your research. If you are not sure, read the appropriate sections before making your selection.

☒ Life sciences ☐ Behavioural & social sciences ☐ Ecological, evolutionary & environmental sciences

Life sciences study design

All studies must disclose on these points even when the disclosure is negative.

Sample size	Appropriate sample sizes were predetermined based on reports in the literature, pilot experiments, or through power analysis.
Data exclusions	One animal was excluded from the alcohol consumption study as the bottle in its cage was leaking. Two rats (one male and one female) were excluded from the final heroin self-administration dataset due to defective catheters. Eight rats were excluded from the final sucrose self-administration dataset due to failure to acquire sucrose self-administration. These exclusions were indicated in the methods. No other data were excluded.
Replication	Details about replication of specific experiments are shown in Supplementary Table 1. All attempts at replication were successful.
Randomization	For cellular assays, treatment groups were always randomized across the plate and analyzed blinded. For animal studies, animal treatments were randomized.
Blinding	All cellular assays and animal work was analyzed by an experimenter blinded to the treatment condition.

Reporting for specific materials, systems and methods

We require information from authors about some types of materials, experimental systems and methods used in many studies. Here, indicate whether each material, system or method listed is relevant to your study. If you are not sure if a list item applies to your research, read the appropriate section before selecting a response.

Materials & experimental systems

n/a	Involved in the study
☐	☒ Antibodies
☐	☒ Eukaryotic cell lines
☒	☐ Palaeontology
☐	☒ Animals and other organisms
☒	☐ Human research participants
☒	☐ Clinical data

Methods

n/a	Involved in the study
☒	☐ ChIP-seq
☒	☐ Flow cytometry
☒	☐ MRI-based neuroimaging

Antibodies

Antibodies used	chicken anti-MAP2 antibody (1:10,000; EnCor, CPCA-MAP2)
Validation	This antibody was validated by the manufacturer by demonstrating selective labeling of neurons in neuron-glia co-cultures and by western blot. It has been utilized in the following papers, among many others: 1. Dehmelt, H and Halpain, S. The MAP2/Tau family of microtubule-associated proteins. Genome Biol. 6:204 (2005). 2. Nunez J. Immature and mature variants of MAP2 and tau proteins and neuronal plasticity. Trends Neurosci. 11:477-9 (1998).

Eukaryotic cell lines

Policy information about cell lines

Cell line source(s)	HEK293 (gift from Craig January, University of Wisconsin, Madison); HEK Flp-In 293 T-Rex stable cell lines (Invitrogen)
Authentication	These cell lines were not authenticated
Mycoplasma contamination	These cell lines were not tested for mycoplasma contamination.
Commonly misidentified lines (See ICLAC register)	N/A

Animals and other organisms

Policy information about studies involving animals; ARRIVE guidelines recommended for reporting animal research

Laboratory animals	The species, strain, sex, and age of animals are reported in the methods where appropriate and included 8 week old, male and female C57BL/6J mice; male and female, 7 dpf zebrafish; male and female, 6 dpf zebrafish; male and female, 6 hpf zebrafish;

	male 9–10 week old C57BL/6J mice; male and female, 12 weeks old C57/BL6J mice; E18 rats (unknown sex); Male and female Thy1-GFP-M line mice (> 8 weeks old); male C57/BL6J mice (6-8 weeks old); male and female Wistar rats (>8 weeks old)
Wild animals	We did not use wild animals.
Field-collected samples	We did not use field-collected samples.
Ethics oversight	All experimental procedures involving animals were approved by either the UCD, UCSF, UCSC or CU Anschutz Institutional Animal Care and Use Committee (IACUC) and adhered to principles described in the National Institutes of Health Guide for the Care and Use of Laboratory Animals. The University of California, Davis (UCD), the University of California, San Francisco (UCSF), the University of California, Santa Cruz (UCSC), and the University of Colorado Denver, Anschutz Medical Campus (CU Anschutz) are accredited by the Association for Assessment and Accreditation of Laboratory Animal Care International (AAALAC).

Note that full information on the approval of the study protocol must also be provided in the manuscript.